Targeting ULK1 and USP20 to modulate autophagy and chemosensitivity in cancer cell lines

TUQA ABU THIAB[1], MALEK ZIHLIF[2], DANA ALQUDAH[3] and AMER IMRAISH[1]

[1]Department of Biological Sciences, School of Science, The University of Jordan, Amman 11942, Jordan;
[2]Department of Pharmacology, School of Medicine, The University of Jordan, Amman 11942, Jordan;
[3]Cell Therapy Center, The University of Jordan, Amman 11942, Jordan

Received October 17, 2025; Accepted February 12, 2026

DOI: 10.3892/br.2026.2124

Abstract. Autophagy is a conserved catabolic process essential for maintaining cellular homeostasis by degrading and recycling damaged organelles and misfolded proteins. In cancer, autophagy plays a dual role, acting as both a tumor suppressor and promoter depending on the stage and context. Unc-51-like kinase 1 (ULK1), a key initiator of autophagy, is tightly regulated by USP20, a de-ubiquitinase that stabilizes ULK1 by preventing its lysosomal degradation. However, their roles in cancer progression and treatment response remain poorly understood. The present study investigated the baseline expression of ULK1 and USP20 across several cancer cell lines and evaluates the effects of their silencing on chemosensitivity. The findings of the present study showed that ULK1 was highly expressed in MCF-7 breast cancer cells and minimally in U87 glioblastoma cells. USP20 showed high expression in MCF-7, MDA-MB-231 and HepG2, and low expression in others. Combined silencing of ULK1 and USP20 with chemotherapy altered drug sensitivity across cancer types. ULK1 knockdown increased drug sensitivity and induced cell death in HepG2, MDA-MB-231 and PanC1 cell lines, but conferred chemoresistance in MCF-7, A549 and U87 cancer cells. Similarly, USP20 silencing sensitized MCF-7, HepG2 and PanC1 cells to chemotherapy, while enhancing survival in U87 cells. These results suggest that ULK1 and USP20 have cancer-type-specific roles in modulating autophagy and chemotherapy response. Targeting these proteins may provide novel therapeutic strategies to overcome chemoresistance and promote apoptosis in cancer treatment.

Correspondence to: Dr Amer Imraish, Department of Biological Sciences, School of Science, The University of Jordan, 19 Queen Rania Al-Abdullah Street, Amman 11942, Jordan
E-mail: a.imraish@ju.edu.jo

Key words: cancer, autophagy, apoptosis, chemosensitivity, Unc-51-like kinase 1, USP20

Introduction

Autophagy is a conserved catabolic process in which cytosolic macromolecules, lipid droplets, labeled proteins, and damaged organelles are recycled via a lysosome-mediated digestion process. This mechanism is normally important for cellular survival and maintenance of energy homeostasis (1). It also establishes cellular adaptations in response to stressful conditions (2). Autophagy is a highly regulated process and can be influenced by aging, oxygen, nutrients and diseases, especially cancers (3).

Promoting autophagy requires the activation of the ULK initiation complex, which is mainly composed of UNC-51-like kinase 1 (ULK1), autophagy-related factor 13 (ATG13), and focal adhesion kinase family interacting protein of 200 kD (FIP200). Once activated, an autophagosome forms to initiate the autophagy process (4,5). ULK complex is under the direct inhibition of the mechanistic target of rapamycin complex 1 (mTORC1), which is highly activated under nutrient-rich conditions (6). On the other hand, the inhibition of mTORC1 over the ULK complex is released under starvation and stressful conditions, which in turn activates autophagy as a survival mechanism (6). Cancer malignant traits, such as increased proliferation and residency in oxygen and nutrient-deprived environments, require alterations in their metabolic activities, enabling cancerous cells to adapt to stressful conditions (7). Among several factors involved in metabolic reprogramming, autophagy has been found to play a crucial role in cancer initiation, progression and chemoresistance (8). The interplay between autophagy and cancer is complicated and contradictory, as it has been previously reported that autophagy plays a bipolar role in cancer progression and operates differently at different stages of cancer progression (9,10). Seemingly, the opposing roles of autophagy are observed in the prevention of early tumor development vs. the maintenance and metabolic adaptation of established and metastasizing tumors to promote cellular survival (11).

Recently, researchers have focused on enhancing tumor sensitivity to chemotherapy by targeting autophagy. However, this approach is complicated by the biphasic role of autophagy in cancer progression; inhibiting it may suppress tumor survival but could also eliminate its tumor-suppressive effects in early stages (2). Therefore, the timing and tumor

context are critical in choosing the appropriate autophagy intervention. In advanced cancers, inhibiting autophagy may be more effective, whereas inducing it in apoptosis-resistant tumors could promote cancer cell death (12). These findings underscore that autophagy-targeted therapies should be personalized, depending on cancer type and stage (2,12). Combination therapies that use autophagy inhibitors, such as hydroxychloroquine or chloroquine, alongside standard anticancer medications, are being assessed in numerous clinical trials (13-15). However, targeting specific molecular nodes within the autophagy pathway, such as ULK1, rather than using nonspecific pharmacological agents, may help minimize adverse effects on normal cells and provide more precise regulation (16).

A growing theory on the variety of ULK1 functions pinpoints its critical role in several non-canonical processes, primarily cellular fate determination, metabolic reprogramming, stress response, and disease development, particularly cancers (17,18). The mitotic delay and increased cell death observed after ULK1 knockdown likely result from both impaired autophagy and ULK1's autophagy-independent roles in mitosis, including regulation of centrosome dynamics, spindle assembly, and proper chromosome segregation, suggesting that defects in cell division may substantially contribute to the phenotype. Based on a previous study, cells are exposed to extreme oxidative stress when ULK1 is inhibited. This is because of the metabolic shifting from glycolysis to the utilization of mitochondrial oxidative phosphorylation as an alternative mechanism (19). Accordingly, LKB1 mutant lung cancer cells are then re-sensitized to overcome chemoresistance by the oxidative phosphorylation associated with ULK1 inhibition (20). On the other hand, Deng *et al* (20) suggested that trametinib, a MAPK1/3 kinase inhibitor, prevents bone metastases in MDA-MB-231 breast cancer (BC) by reestablishing mitophagy function through upregulating ULK1 activity. Away from its role in autophagy induction, ULK1 has also been demonstrated to influence chromosomal segregation and mitotic spindle organization during cell division. Thereafter, inhibition of ULK1 resulted in defective chromosome alignment and delayed mitosis. This suggests that ULK1 controls mitotic integrity, which is essential for the advancement of the cell cycle and the proliferation of cancer cells (21).

The ability of cancer cells to orchestrate autophagy flux is extended beyond the genetic expression of autophagy-related genes via several epigenetic and posttranslational modification mechanisms, including ubiquitination and de-ubiquitination processes (7). Several autophagy-related factors were found to be either ubiquitinated or de-ubiquitinated in favor of cancer development and spread. Interestingly, distinct cancer types express distinct ubiquitination/de-ubiquitination enzymes, and different tissue types have varied roles for these enzymes. Accordingly, it has been shown that activated ULK1 (or ULK-1) is further stabilized, and the basal level of autophagy is maintained when the de-ubiquitination peptidase USP20 removes ubiquitin from it, thereby preventing its degradation. Moreover, USP20 upregulation was found to be associated with various cellular biological processes such as cell cycle progression, proliferation, migration and invasion, playing a pivotal role in tumorigenesis (22). It has been hypothesized that under prolonged starvation, the interaction between USP20 and ULK1 is reduced to terminate autophagy, a protective response that drives the cell away from apoptosis (22). These data suggest that modulating proteolytic ubiquitination of ULK1 via USP20 may be effective to bypass cancerous chemoresistance and may play a role in deciding cellular fate, based on the fact that persistent enhancement of autophagy could be a successful strategy that drives cellular death and apoptosis in different cancer types and sensitizes tumors to chemotherapeutic drugs.

As a mechanism that may be directly or indirectly involved in deciding the fate of the cell, either survival or death (3), it is necessary to ascertain where and when autophagy contributes to or inhibits tumor development and progression in different cancer types. This is fundamental to establish autophagy as a potential therapeutic target for personalized medication in different cancer types. Moreover, understanding the dynamic conversion between ubiquitination and de-ubiquitination status in different cancer types, especially those related to the autophagy process, may provide novel insights and new treatment candidates for cancer therapy strategies. In the current study, it was aimed to perform this task by measuring levels of basal autophagy flux in different human cancer cell lines. Furthermore, a new system for selective inhibition of autophagy was established using siRNA gene silencing technology for both ULK1 and USP20, to evaluate the potential role of autophagy inhibition on the fate of different cancer types when combined with conventional therapeutic agents. This system will also be evaluated for its efficiency in sensitizing different multi-drug-resistant cancer types to their selective commercially available chemotherapeutic drugs.

Materials and methods

Cell culture and maintenance. The following cell lines were involved in the present study and provided from The American Type Culture Collection, human pancreatic cancer cell line PANC-1 (CRL-1469™), Human lung carcinoma-A549 (CRM-CCL-185™), human glioblastoma of unknown origin U-87 MG (HTB-14™), human liver cancer HepG2 (HB-8065™), human breast carcinoma MCF7 (HTB-22™), human breast adenocarcinoma MDA-MB-231 (CRM-HTB-26™), and human normal primary non-immortalized dermal fibroblasts-HDFa (PCS-201-012, https://www.atcc.org/products/pcs-201-012).

As instructed by the supplier, PANC-1, A549, MDA-MB-231, U-87, Fibroblasts and HepG2 cells were cultured in Dulbecco's Modified Eagle Medium (cat. no. ECB7501L; Euroclone SpA), while the MCF-7 cell line was cultured in RPMI-1640 culture medium (cat. no. ECB9006L; Euroclone SpA). To prepare a complete medium for the aforementioned cells, 10% heat-inactivated fetal bovine serum (FBS; cat. no. 26170043; Gibco; Thermo Fisher Scientific, Inc.), 1% of 200 mM L-Glutamine (cat. no. ECB3000D; Euroclone SpA), 1% of 1M HEPES buffer (cat. no. ECM0180; Euroclone SpA), and 1% of 100X penicillin-streptomycin (cat. no. ECB3001; Euroclone SpA) were added to the media. Cultured cells were passaged in a humidified incubator at 37˚C with 5% CO_2 until being used for subsequent experiments.

Autophagy basal level in different cell lines using the reverse transcription-quantitative (RT-q) PCR technique. To investigate the baseline level of autophagy flux in different cancer cell lines, the expression levels of ULK1 and USP20 de-ubiquitinase enzyme were precisely measured. A total of $5x10^5$ of each cell type was subjected to RNA extraction using the extraction buffers provided by the RNeasy Plus Mini Kit (Qiagen GmbH). The amount of 1,000 ng of RNA was converted to complementary DNA (cDNA) using the PrimeScript 1st strand cDNA Synthesis Kit (Takara Bio, Inc.). Then, qPCR was performed using Applied Biosystems™ PowerTrack™ SYBR Green Master Mix (Thermo Fisher Scientific, Inc.). Thermocycling conditions were started with the initial activation at 95˚C for 2 min, followed by 40 cycles of denaturation at 95˚C for 15 sec and annealing/extension at 60˚C for 1 min. The sequence of forward and reverse primers used in this experiment is listed in Table I. The 18S rRNA was used as an internal control of the experiment. The baseline expression of ULK1 and USP20 of each cell line was calculated relative to their expression in normal fibroblast cells. Relative ULK1 and USP20 expression levels were quantified using $2^{-\Delta\Delta Cq}$ method (23), and further statistical analysis was performed using GraphPad Prism software 9 (Dotmatics).

Knockdown of ULK1 and USP20 genes using siRNA gene silencing therapy. To evaluate the differential response of different cancer cells to autophagy inhibition, cells were transfected with siRNAs to knockdown both ULK1 and USP20 mRNAs. Lipoplexes were prepared by mixing each siRNA type: siULK1 (cat no. 5185429; Microsynth AG), siUSP20 (cat no. 5185431; Microsynth AG), and siSCR (scrambled negative control siRNA) (cat no. 5185433; Microsynth AG), with Lipofectamine™ RNAiMAX Transfection Reagent (cat no. 18324012, Gibco; Thermo Fisher Scientific, Inc.) in a serum-free medium. Custom siRNAs were synthesized by Microsynth AG (https://www.microsynth.com/home-ch.html), and the sequence of each siRNA is indicated in Table II. Four different concentrations of each siRNA lipoplex were prepared: 200, 100, 50 and 25 nM. A transfection experiment was performed by plating $200x10^3$ of each cell type into a 12-well plate and then kept overnight in the incubator at 37˚C to firmly adhere. The day after, cells were transfected with each concentration of lipoplexes in triplets and transfected cells were starved for 6 h, then the medium was adjusted to contain 10% FBS to end the starvation. Control untreated cells were running alongside the experiment and subjected only to starvation, like the transfected cells. After a total of 24-h of incubation with lipoplexes, cells were harvested for RNA extraction using the RNeasy Plus Mini Kit (Qiagen). knockdown efficiency of siULK1 and siUSP20 for both ULK1 and USP20 mRNAs was confirmed via the qPCR technique. ULK1 and USP20 primers were previously mentioned in the table and 18SrRNA was used as an internal control. ΔΔCT values were calculated using Microsoft Excel software, and subsequent significant inhibition was analyzed using one-way ANOVA followed by Bonferroni's multiple comparisons post hoc test, GraphPad Prism software 9 (Dotmatics). All siRNA knockdown experiments included a well-validated scrambled siRNA control to account for potential off-target effects or innate immune activation. Experimental outcomes, including IC_{50} measurements, were analyzed relative to siSCR-treated cells to ensure that observed effects reflect specific gene silencing.

Table I. List of primers used for quantitative PCR.

Gene name	Primer sequence (5'-3' direction)
ULK1	F: CCATCCCAGTCCCCACGCAG
	R: GCGGATGGCAGAGGACCGAG
USP20	F: CAGTTGCGAGTGCAGGCTC
	R: TGACACGAAGCCCACAGGAA
P62	F: CGCACTACCGCGATGAGGAC
	R: TGTCATCCTTCACGTAGGACATGG
Bcl-2	F: GGACAACATCGCCCTGTGGA
	R: TCCACAAAGGCATCCCAGCC
18S rRNA	F: AGAAACGGCTACCACATCCA
	R: TACAGGGCCTCGAAAGAGTC
Bax	F: GGTCCGGGGAGCAGC
	R: GATCCTGGATGAAACCCTGAAG

F, forward; R, reverse.

Table II. List of siRNA sequences used to knockdown ULK1 and USP20 mRNAs.

Target gene	siRNA sequences (5'-3' direction)
ULK1	sense: GCUGGGGAAGGAAAUCAAA
	antisense: UUUGAUUUCCUUCCCCAGCag
USP20	sense: GGACAAUGAUGCUCACCUA
	antisense: UAGGUGAGCAUCAUUGUCCgg
Negative control (scramble)	sense: UUCUCCGAACGUGUCACGUTT
	antisense: AAACGUGACACGUUCGGAGAA

siRNA, small interfering RNA.

Effect of ULK1 and USP20 knockdown on chemoresistance to several chemotherapeutic drugs. After determining the efficient knockdown concentration of siULK1, siUSP20 and siSCR, different cancer types were treated with a selective chemotherapeutic drug along with the aforementioned siRNAs mentioned above. The chosen chemotherapeutic agents were as follows: Gemcitabine for the treatment of PANC-1, while HepG2, U-87, MCF-7 and MDA-MB-231 were treated with Doxorubicin. A549 lung cancer cells were treated with Cisplatin. Normal fibroblasts were treated with the three chemotherapeutic agents, gemcitabine, doxorubicin and cisplatin. Briefly, different cell types were seeded into a 96-well plate with a seeding density of $7x10^3$. Next, lipoplexes at a certain concentration of each siRNA type (Table III) were prepared as previously indicated and applied to cells. After 6 h of incubation at 37˚C with lipoplexes, a serial dilution of each chemotherapeutic agent was then applied over

Table III. Selected safe and effective concentrations of siRNAs over each cell type.

Cell type	siULK1	siUSP20	siSCR
Fibroblast	25 nM	25 nM	25 nM
HepG2	200 nM	100 nM	25 nM
A549	25 nM	25 nM	25 nM
PanC1	50 nM	200 nM	25 nM
U87	200 nM	100 nM	25 nM
MDA-MD-231	200 nM	100 nM	25 nM
MCF-7	25 nM	200 nM	25 nM

A triplicate of each siRNA treatment group was considered for this experiment. One-way ANOVA was performed to statistically analyze the significant changes. si-, small interfering.

the cells. The serial dilution of each chemotherapy started from 100 μM down to 15 concentrations. After 72 h, MTT assay was performed following the manufacturer's protocol of CellTiter 96® Non-Radioactive Cell Proliferation Assay (Promega Corporation) to measure the cytotoxicity. After 3 h of incubation with the provided MTT reagent, purple formazan crystals were dissolved by the provided stop solution containing dimethyl sulfoxide, and the optical density values were measured at 570 nm. Cells treated with chemotherapy only, siRNA only, or untreated at all were running alongside the experiment as experimental controls. GraphPad Prism 9 software (Dotmatics) was used to calculate the half-maximal inhibitory concentration-IC_{50} values for each treatment group using the logarithmic trend line of cytotoxicity graphs [log (concentration vs. inhibition)].

Effect of chemotherapy alone/siRNAs alone on autophagy flux and apoptosis via qPCR. To evaluate the efficiency of combination therapy over cell fate, it was mandatory to evaluate the effect of each chemotherapy alone on autophagy flux, LC3B and P62, and apoptosis-related genes, Bax and Bcl-2. Moreover, the effect of knocking down ULK1 and USP20 on apoptosis-related genes was important to be studied. For this purpose, 100,000 cells of each cancer cell type were seeded in a 12-well plate, then they were treated with the corresponding chemotherapy, siULK1, siUSP20, or siSCR as mentioned in the previous sections. Three concentrations of each chemotherapy were selected for this experiment, based on the IC_{50} values of each chemotherapy for each cell line. The concentrations of each siRNA that have been applied in this experiment are listed in Table III. Treated cells were cultured for 24 h at 37˚C, then total RNA was extracted as aforementioned. qPCR was performed to test the changes in the expression of autophagy flux genes, LC3B and P62, and apoptosis-related genes, Bax and Bcl-2. The 18S rRNA gene was used as a reference gene in this experiment. Primer sequences that have been used are listed in Table I.

Assessment for cellular fate after combination therapy via flow cytometry. The ability of combination therapy to induce apoptosis in treated cancerous cells was investigated, and this was performed by treating $1x10^5$ of each cancer type with the selected siRNA concentration (Table III) and two concentrations of each selected chemotherapy. A period of 24-h treatment was ended by harvesting the cells, followed by staining with TACS® Annexin V-FITC Apoptosis Detection Kit (R&D Systems, Inc.). Apoptosis was detected and analyzed using BD FACSCanto™ II Flow Cytometer, coupled with BD FACS Diva software (BD Biosciences). Statistical analysis was done using one-way ANOVA followed by Bonferroni's multiple comparisons post hoc test (Dotmatics).

Statistical analysis. The IC_{50} values were determined using the logarithmic trend line of cytotoxicity graphs [log (concentration vs. inhibition)] in GraphPad Prism 8 software (Dotmatics). All the experiments were performed in triplicate, and the mean ± SEM was used to display the data. Data were analyzed using one-way ANOVA followed by Bonferroni's multiple comparisons post hoc test. $P<0.05$ was considered to indicate a statistically significant difference.

Results

Baseline expression of autophagy markers via qPCR. ULK1, an important component of the autophagy initiation complex, showed different expression levels in various cancer types based on qPCR data (Fig. 1A). The triple-negative MDA-MB-231 cell line had a low level of ULK1 compared with normal fibroblasts. By contrast, MCF7 BC cells had the highest ULK1 expression. Additionally, U87 glioma cells exhibited the lowest ULK1 expression among all the examined cells when compared with normal fibroblasts (Fig. 1A). A549 and Panc1 also showed low levels of ULK1 expression, at nearly half the level found in fibroblasts. HepG2 cells demonstrated a slight decrease in ULK1 expression compared with normal fibroblasts.

Different cell lines also varied in their levels of USP20 expression (Fig. 1B). USP20 levels in BC cell lines were similar to those in normal fibroblasts, though it was very low and nearly absent in lung and pancreatic cancer cell lines. In U87 cells, there was a significant decrease in USP20 expression compared with normal cells. Finally, the USP20 levels in HepG2 cells were slightly lower than those in normal cells.

Knockdown of ULK1and USP20 genes using siRNA gene silencing therapy. Gene silencing technology was used on the tested cancer cell lines to modify autophagy. For each type of cancer cell, four different siULK1 and siUSP20 concentrations were tested. As shown in Table III, the concentrations that led to a significant and effective suppression of both genes varied among the different cells. This suggests that different cell types respond differently to these silencing molecules and the level of lipoplex absorption also varies among the cell types. The concentrations of both siRNAs listed in Table III were considered for each cell type in the following experiments. The lowest tested concentration of scrambled siRNA (25 nM) was used for all experiments. This concentration should not show any significant effect compared with the others.

To verify the efficiency of gene silencing, ULK1 and USP20 mRNA expression was assessed in cells transfected with their respective knockdown constructs using RT-qPCR.

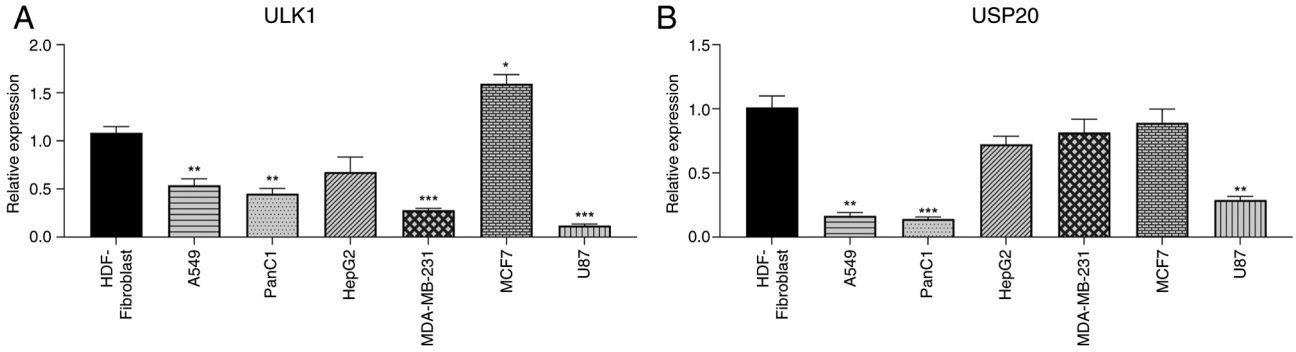

Figure 1. Baseline expression of ULK1 and USP20 in different cancer cell line. Triplicates of normal untreated cells were harvested, and the level of expression was determined using the reverse transcription-quantitative PCR technique. (A) Differential expression of ULK1 in each cancer cell line relative to its expression in normal fibroblasts. (B) Differential expression of USP20 in each cancer cell line relative to its expression in normal fibroblasts. Data are presented as the mean ± SEM. Statistical significance was indicated as *P<0.05, **P<0.01 and ***P<0.001 (one-way ANOVA followed by Bonferroni's multiple comparisons post hoc test). ULK1, Unc-51-like kinase 1.

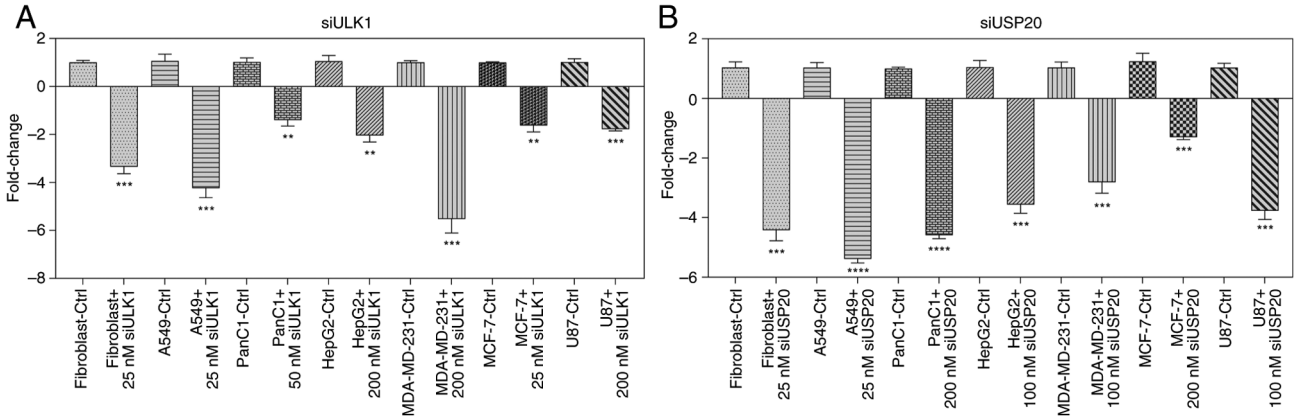

Figure 2. Gene expression of ULK1 and USP20 genes after treatment with Lipofectamine coated siRNAs via reverse transcription-quantitative PCR. (A) Fold change in the expression of ULK1 after treatment with Lipofectamine-coated siULK1 at different concentrations on cancer cells. (B) Fold change in the expression of USP20 after the treatment with Lipofectamine-coated siUSP20 at different concentrations on cancer cells. Statistical significance was indicated as **P<0.01, ***P<0.001 and ****P<0.0001. ULK1, Unc-51-like kinase 1; si-, small interfering.

As shown in Fig. 2A and B, ULK1- and USP20-specific siRNA significantly reduced transcript levels compared with cells transfected with the non-targeting control. These results confirmed successful and specific knockdown of ULK1 and USP20 under the experimental conditions used.

The marked differences in siRNA potency across cell lines are explained by intrinsic variations in transfection efficiency, basal target gene expression, mRNA stability, RISC loading capacity, endosomal escape and cell proliferation rates. These biological and biophysical factors collectively determine the concentration of siRNA required in each cell type to achieve efficient ULK1 or USP20 silencing.

Effect of ULK1 and USP20 knockdown on chemoresistance to several chemotherapeutic drugs. The possibility of shifting cancer cells' sensitivity to conventional chemotherapy upon the knockdown of ULK1 and USP20 was tested using MTT assay. The results were interesting and responses varied across different cell lines and even within the same cell line when different genes were involved (Table IV). The table lists the IC_{50} values for each chemotherapy used and those obtained from combining chemotherapy with various siRNAs. Normal fibroblast cells showed significant toxicity from cisplatin, gemcitabine and doxorubicin. Adding siULK1 and siUSP20 to cisplatin-treated fibroblasts offered slight protection from the drug's toxic effects, but this was not significant. Notably, the IC_{50} value for fibroblasts treated with siULK1 and gemcitabine (24.85 μM) was nearly 4-fold higher than that for fibroblasts treated with gemcitabine alone (6.38 μM). This indicates that siULK1 protects normal fibroblasts from the drug's harmful effects. Additionally, silencing USP20 led to a slight and insignificant increase in the IC_{50} of gemcitabine-treated fibroblasts. By contrast, adding siULK1 to doxorubicin-treated fibroblasts had no significant effects, but including siUSP20 increased doxorubicin toxicity compared with fibroblasts treated with doxorubicin alone.

MCF-7 and MDA-MB-231 BC cell lines responded differently to the knockdown of USP20 and ULK1. When siULK1 was added to MCF-7 treated with doxorubicin, their resistance to the drug increased by more than 2-fold (IC_{50}=0.32 μM) compared with chemotherapy-treated group (IC_{50} value equals 0.14 μM). By contrast, siUSP20 significantly increased their sensitivity to the drug by more than 3-fold (IC_{50}=0.04 μM). Unlike MCF-7 cells, MDA-MB-231 cells became more

Table IV. IC50 values of various cancer cell lines treated with chemotherapy alone or in combination with siULK1 or siUSP20.

Cell type	Chemotherapy type	IC_{50} (μM) of Chemotherapy only ± SD	IC_{50} (μM) of Chemotherapy and siULK1 ± SD	P-value	IC_{50} (μM) of Chemotherapy and siUSP20 ± SD	P-value	IC_{50} (μM) of Chemotherapy and siSCR ± SD	P-value
Fibroblast	Cisplatin	54.02±2.46	57.94±5.34	0.31	63.11±11.76	0.26	79.35±12.68	0.09
	Gemcitabine	6.38±1.27	24.85±5.59	0.009[b]	8.17±1.51	0.24	4.67±1.12	0.15
	Doxorubicin	0.30±0.076	0.28±0.01	0.69 ns	0.29±0.011	0.81	0.23±0.02	0.23
MCF-7	Doxorubicin	0.14±0.01	0.32±0.01	0.0001[c]	0.04±0.008	0.0004[c]	0.10±0.02	0.0373[a]
HepG2	Doxorubicin	0.28±0.02	0.09±0.02	0.0003[c]	0.17±0.04	0.013[a]	0.20±0.05	0.048[a]
A549	Cisplatin	11.23±0.69	18.71±1.95	0.003[b]	8.63±1.57	0.057	10.64±0.20	0.22
PanC1	Gemcitabine	2.70±0.28	2.10±0.25	0.0534	1.64±0.35	0.013[a]	2.82±0.58	0.76
U87	Doxorubicin	0.04±0.02	0.11±0.01	0.005[b]	0.10±0.02	0.01[a]	0.08±0.01	0.03
MDA-MB-231	Doxorubicin	0.33±0.05	0.17±0.02	0.004[b]	0.32±0.04	0.79	0.32±0.02	0.75

Three repeats were considered for each treatment group to calculate the IC_{50}. One-way ANOVA followed by Bonferroni's multiple comparisons post hoc test was performed to compare the IC_{50} of each combination therapy group with the IC_{50} of chemotherapy only treated group. Statistically significant results were considered as [a]P<0.05, [b]P<0.01, [c]P<0.001. Si, small interfering.

sensitive to doxorubicin with siULK1 addition (IC_{50}=0.17 μM). USP20 knockdown had no noticeable effect on MDA-MB-231 cells treated with doxorubicin, and the IC_{50} remained close to that of the cells treated with the drug alone.

In HepG2 cells treated with doxorubicin, knocking down ULK1 and USP20 significantly re-sensitized the cells to the drug, with IC_{50} of 0.09 and 0.17 μM, respectively, when compared with doxorubicin-treated HepG2 cells (IC_{50}=0.28 μM). PanC1 cells treated with gemcitabine displayed a similar pattern, becoming more sensitive to the drug; however, the effect of ULK1 inhibition was minimal and statistically insignificant (P=0.053). A549 cells treated with cisplatin revealed more aggressive behavior when ULK1 was inhibited, but those cells were slightly re-sensitized to the drug when USP20 was inhibited. The response of glioblastoma U87 cells to siULK1 and siUSP20 was similar; the cells became more aggressive and resistant to doxorubicin with both knockdowns. Overall, the present findings suggested that selectively inhibiting either USP20 or ULK1 could help re-sensitize cancer cells to standard chemotherapy in different cancer types. Thus, inhibiting USP20 or ULK1 may be beneficial for some cancer types, but it should be avoided for others to improve therapy effectiveness.

Effect of chemotherapeutic agents on autophagy flux. To determine whether traditional chemotherapeutic drugs involve autophagy or other mechanisms, the effect of these agents on the basal levels of autophagy-related genes in different cancer types was assessed. A total of 3 different concentrations of each drug were selected in these experiments, based on the IC_{50} values reported in Table IV. For this purpose, changes in the expression of three autophagy-related genes: ULK1, USP20 and P62 were investigated. As demonstrated in Fig. 3, in HepG2 cells, doxorubicin reduced ULK1 expression in a dose-dependent manner, while P62 expression was increased in a dose-dependent manner. The drug did not significantly affect USP20 expression in HepG2 cells. U87 exhibited a similar response, but the changes were more pronounced. USP20 was also decreased in these cells in a dose-dependent manner. These results suggest that doxorubicin inhibits autophagy flow in these cells to some extent.

The BC cell lines MCF-7 and MDA-MB-231 reacted differently to doxorubicin. Following doxorubicin treatment, ULK1 and USP20 expression changed very little and not significantly in both cell lines. Additionally, P62 expression barely changed in MCF-7 but rose sharply in the more aggressive MDA-MB-231 cell line (Fig. 3). Interestingly, the highest concentration of doxorubicin did not noticeably affect ULK1, USP20, or P62 expression in normal fibroblast cells, but lower doses significantly boosted their expression.

In A549 cells, the highest cisplatin concentration significantly raised USP20 mRNA levels without affecting the autophagy-related genes ULK1 and P62 (Fig. 4A-C). Lower concentrations of cisplatin increased ULK1 mRNA levels but did not have a significant impact on USP20 and P62 mRNA levels. The maximum concentration of cisplatin did not significantly change mRNA levels in fibroblast cells (Fig. 4D-F). However, fibroblasts showed an increase in mRNA levels of all three examined genes with lower concentrations of cisplatin.

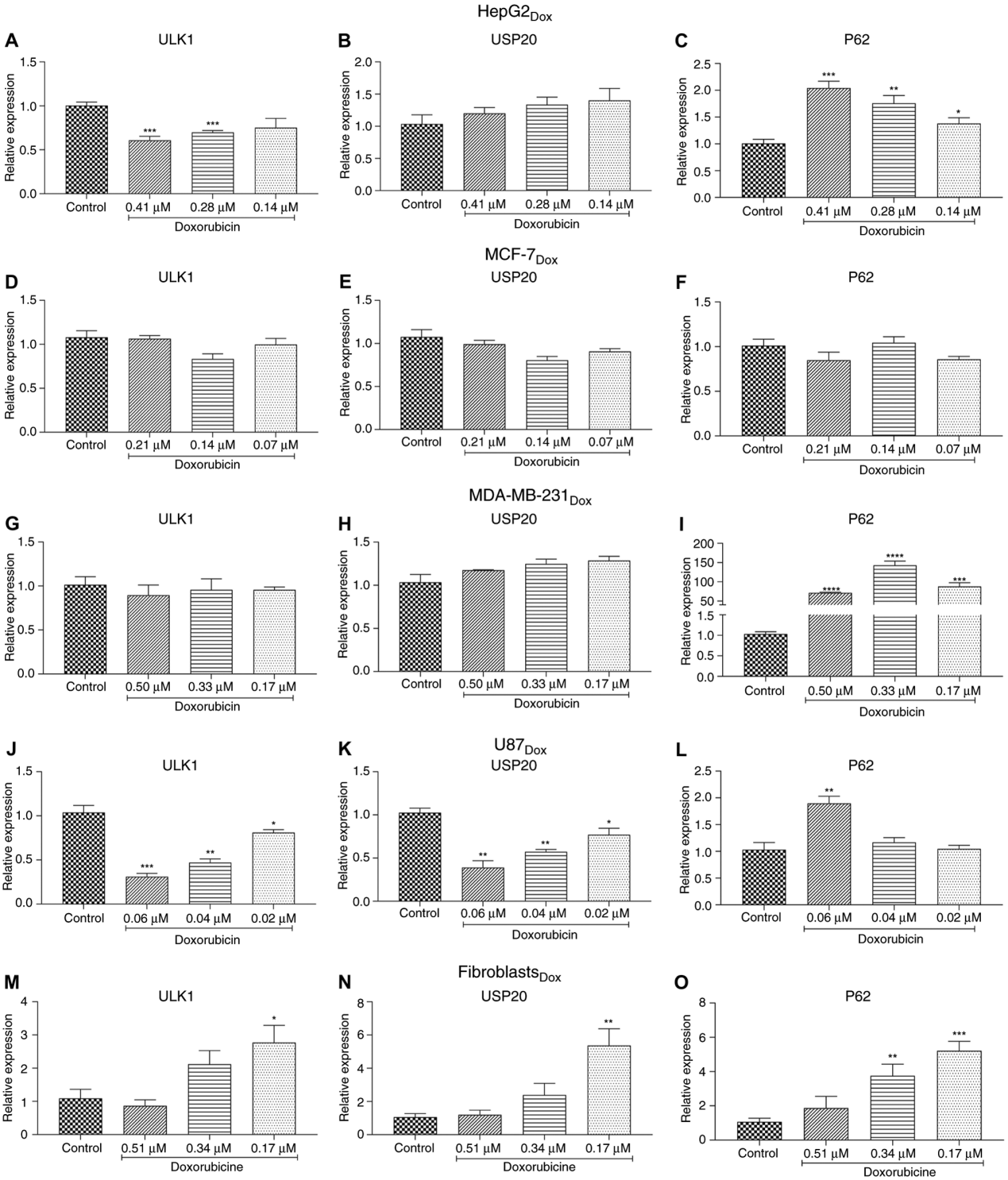

Figure 3. Changes in the basal autophagy flux in different cancer cell lines in response to doxorubicin. HepG2, MCF-7, MDA-MB-231, U87 and normal fibroblast cells were treated with different concentrations of doxorubicin chemotherapy. The level of expression of ULK1, USP20, and P62 was determined *via* reverse transcription-quantitative PCR. (A-C) Relative expression of ULK1, USP20 and P62 in HepG2 cells. (D-F) Relative expression of ULK1, USP20 and P62 in MCF-7 breast cancer cells. (G-I) Relative expression of ULK1, USP20 and P62 in MDA-MB-231 breast cancer cells. (J-L) Relative expression of ULK1, USP20 and P62 in U87 cells. (M-O) Relative expression of ULK1, USP20 and P62 in normal fibroblast cells. Three repeats were considered for each treatment group. Data are presented as the mean ± SEM. Statistical significance was indicated as *P<0.05, **P<0.01, ***P<0.001 and ****P<0.0001 (one-way ANOVA followed by Bonferroni's multiple comparisons post hoc test). ULK1, Unc-51-like kinase 1.

Similarly, gemcitabine treatment increased mRNA levels of ULK1 and P62 in both PanC1 and normal fibroblast cells (Fig. 5). Notably, PanC1 malignant cells showed reduced USP20 expression after exposure to gemcitabine, while normal fibroblast cells exhibited a significantly higher level of it (Fig. 5B and E).

Effect of chemotherapeutic agents and siRNA treatments on apoptosis via RT-qPCR. By tracking changes in the expression of apoptosis-related genes, primarily Bax and Bcl-2, it was possible to identify whether certain chemotherapeutic drugs and siRNAs may lead to apoptosis (Tables V and VI).

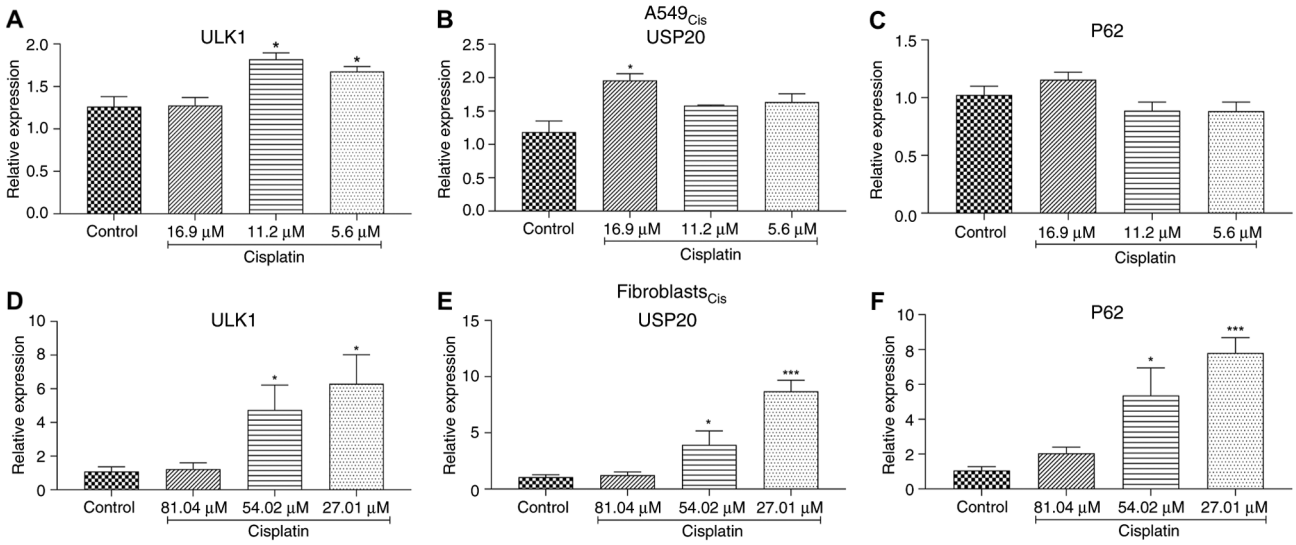

Figure 4. Changes in the basal autophagy flux in A549 lung cancer cells and normal fibroblasts in response to cisplatin chemotherapy treatment. Cells were treated with different concentrations of cisplatin chemotherapy. The level of expression of ULK1, USP20 and P62 was determined via reverse transcription-quantitative PCR. (A-C) Relative expression of ULK1, USP20, and P62 in A549 lung cancer cells. (D-F) Relative expression of ULK1, USP20 and P62 in normal fibroblast cells. Three repeats were considered for each treatment group. Data are presented as the mean ± SEM. Statistical significance was indicated as *P<0.05 and ***P<0.001 (one-way ANOVA followed by Bonferroni's multiple comparisons post hoc test). ULK1, Unc-51-like kinase 1.

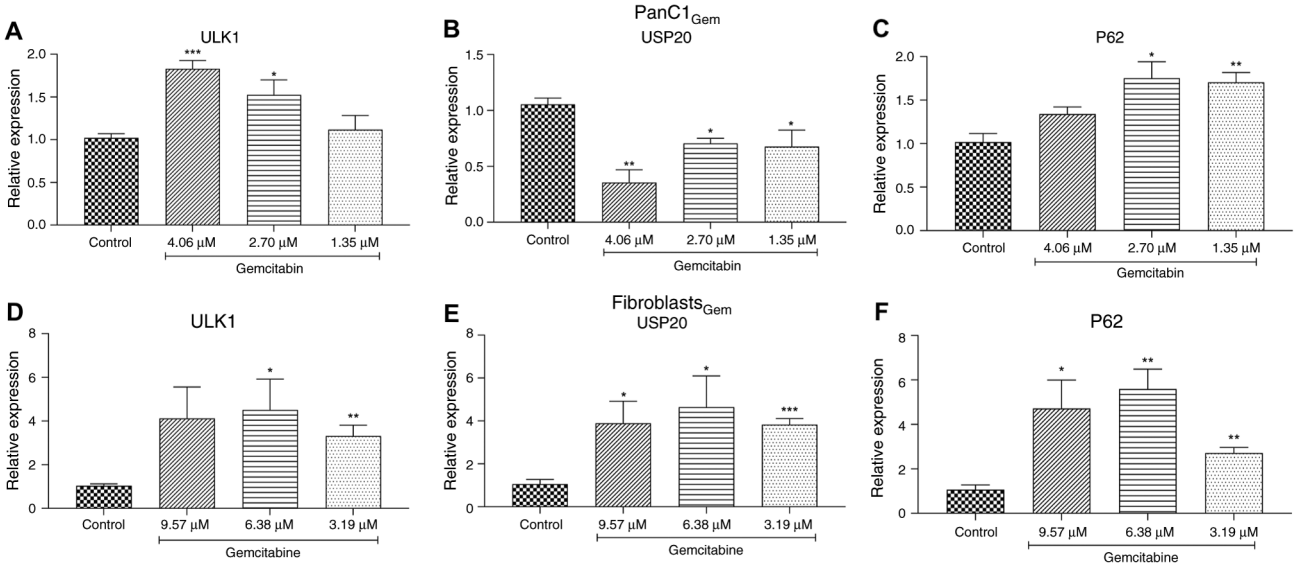

Figure 5. Changes in the basal autophagy flux in PanC1 pancreatic cancer cells and normal fibroblasts in response to gemcitabine chemotherapy treatment. Cells were treated with different concentrations of gemcitabine chemotherapy. The level of expression of ULK1, USP20 and P62 was determined via reverse transcription-quantitative PCR. (A-C) Relative expression of ULK1, USP20 and P62 in PanC1 pancreatic cancer cells. (D-F) Relative expression of ULK1, USP20 and P62 in normal fibroblast cells. Three repeats were considered for each treatment group. Data are presented as the mean ± SEM. Statistical significance was indicated as *P<0.05, **P<0.01 and ***P<0.001 (one-way ANOVA followed by Bonferroni's multiple comparisons post hoc test). ULK1, Unc-51-like kinase 1.

To observe if a cell will trigger or resist apoptosis in response to chemotherapy or siRNA treatment, the ratio of Bax to Bcl-2 expression was precisely measured. A ratio greater than 1 indicates a higher expression of the pro-apoptotic factor Bax, which promotes apoptosis. By contrast, a ratio less than one indicates a greater expression of the anti-apoptotic factor Bcl-2, making cells resistant to treatment. Among all the tested cells, cisplatin and gemcitabine caused significant induction of apoptosis in A549 and PanC1 cells, scoring ratios of 36.9 and 30.2, respectively, for the highest concentration of the drugs, and this effect was dose dependent (Table V). Notably, cisplatin works on A549 by reducing the expression of the anti-apoptotic Bcl-2 gene and slightly increasing the pro-apoptotic gene Bax. Gemcitabine acts on PanC1 by promoting the expression of the pro-apoptotic gene Bax. In both instances, the ratio of Bax to Bcl-2 favors the induction of apoptosis in these cells.

HepG2 cells appeared resistant to apoptosis when exposed to doxorubicin, scoring a 0.56 ratio with the highest tested concentration, and the ratio decreased with

Table V. Bax: Bcl-2 ratio in different cell types after treatment with different doses of chemotherapeutic agents.

Cell line	Chemotherapy type	Chemotherapy concentration	$\Delta\Delta Ct_{Bax} \pm SD$	$\Delta\Delta Ct_{BcL2} \pm SD$	$\Delta\Delta Ct_{Bax:}$ $\Delta\Delta Ct_{BcL2}$ Ratio
Fibroblast	Cisplatin	81.04	2.09±0.86	0.54±0.85	3.9
		54.02	2.6±1.2	0.30±1.2	8.7
		27.01	6.9±2.4	0.23±2.3	30.5
Fibroblast	Gemcitabine	9.57	6.9±2.9	2.6±2.5	2.6
		6.38	10.6±4.8	5.04±5.6	2.1
		3.79	4.6±1.4	3.2±3.06	1.5
Fibroblast	Doxorubicin	0.51	0.99±0.13	0.58±0.61	1.7
		0.34	0.68±0.36	4.3±5.3	0.16
		0.17	2.09±0.73	0.67±0.63	3.1
MCF-7	Doxorubicin	0.21	3.2±1.1	1.1±1.1	2.9
		0.14	1.9±0.31	1.3±1.3	1.5
		0.07	1.3±0.6	1.4±1.4	0.92
HepG2	Doxorubicin	0.41	0.76±0.19	1.35±1.5	0.56
		0.28	0.62±0.23	2.01±2.07	0.31
		0.14	0.43±0.25	2.2±2.06	0.19
A549	Cisplatin	16.9	2.9±0.31	0.08±0.06	36.9
		11.2	2.7±0.95	0.07±0.08	37.5
		5.6	2.7±1.2	0.41±0.44	6.6
PanC1	Gemcitabine	4.06	31.9±0.35	1.05±1.07	30.2
		2.7	39.4±1.1	1.3±1.26	31.03
		1.35	32.3±2.9	1.4±1.37	23.04
U87	Doxorubicin	0.06	1.5±0.46	1.2±1.05	1.2
		0.04	1.3±0.27	0.82±0.85	1.6
		0.02	1.08±0.26	0.92±0.91	1.18
MDA-MB-231	Doxorubicin	0.5	1.03±0.01	0.52±0.51	1.99
		0.33	1.5±0.59	0.91±0.91	1.64
		0.17	1.9±0.2	1.19±1.22	1.58

A triplicate of each treatment group was considered for this experiment. Student's t-test was performed to statistically analyze the significant changes.

lower concentrations. This may indicate that the cellular sensitivity toward doxorubicin is adapted by pathways other than Bax-driven apoptosis. Similar to A549 and PanC1, other cell types, including U87, MDA-MB-231, MCF-7 and normal fibroblasts, induced apoptosis when treated with the appropriate chemotherapy, but to a much lesser degree (Table V).

Silencing ULK1 led to the induction of apoptosis in HepG2, PanC1, MDA-MB-231 and normal fibroblast cells. However, MCF-7, A549 and U87 showed the opposite response; ULK1 knockdown made them more resistant to apoptosis (Table VI). Furthermore, USP20 silencing changed cellular fate, as HepG2, PanC1 and U87 cancer cells underwent apoptosis following USP20 knockdown (Table VI). It is noteworthy that normal fibroblast cells had a strong response to USP20 knockdown and underwent apoptosis when treated with siUSP20. Other cell types, specifically MCF-7, A549 and MDA-MB-231, were protected from apoptosis (Table VI), which may lead these cells to develop aggressive and resistant traits when lacking USP20 activity.

Notably, the high standard deviations in Bax: Bcl-2 ratios, such as in PanC1 cells treated with gemcitabine, likely reflect biological heterogeneity and transient fluctuations in mRNA expression during apoptosis, as well as technical variability in mRNA quantification.

Assessment for cellular fate after combination therapy via flow cytometry. The initial findings about how each chemotherapy or siRNA affects apoptosis are controversial. For example, HepG2 cells became resistant to apoptosis when treated with chemotherapy. However, they induced apoptosis when ULK1 was suppressed with siULK1. This raises questions about the fate of the cells, if they would survive or die after combining the two treatments. To explore how cells respond to combination therapy, an apoptosis assay was performed. Two concentrations of chemotherapy were applied to each cell type, either alone or with siULK1 or siUSP20. This assay focused on four populations: healthy cells, necrotic cells, early apoptotic cells and late apoptotic cells. The distribution of each population for each treatment group is displayed as a percentage in

Table VI. Bax: Bcl-2 ratio in different cell types after the treatment with siULK1 or siUSP20.

Cell type	siRNA Conc. (nM)	$\Delta\Delta Ct_{Bax}$ ± SD	$\Delta\Delta Ct_{Bcl-2}$ ± SD	$\Delta\Delta Ct_{Bax}$: $\Delta\Delta Ct_{Bcl-2}$ Ratio
Fibroblast	25-siULK1	21.7±6.6	1.08±0.05	19.9
	25-siUSP20	83.4±1.8	3.03±0.003	27.5
MCF-7	25-siULK1	0.8±0.4	1.1±0.5	0.68
	200-siUSP20	0.8±0.07	1.2±0.7	0.67
HepG2	200-siULK1	7.7±4.3	1.2±1.2	6.3
	100-siUSP20	1.2±0.3	0.41±0.5	2.9
A549	25-siULK1	0.25±0.07	1.1±0.2	0.22
	25-siUSP20	0.18±0.03	0.55±0.3	0.33
PanC1	50-siULK1	16.5±2.05	3.7±3.9	4.5
	200-siUSP20	0.9±0.2	0.41±0.5	2.2
U87	200-siULK1	0.21±0.2	0.42±0.2	0.5
	100-siUSP20	17.9±1.1	5.8±3.2	3.1
MDA-MB-231	200-siULK1	0.2±0.01	0.07±0.05	2.2
	100-siUSP20	0.05±0.06	0.18±0.1	0.29

Each treatment group displays the results of three experimental repeats. si-, small interfering.

Table VII and Figs. S1-S9. For data analysis, each concentration of chemotherapy with siRNA was compared with the same concentration of chemotherapy alone.

The results revealed that doxorubicin causes cell death by activating necrosis (accounting for ~30.25%) instead of apoptosis (accounting for only ~8.45%), leading to a decrease in the healthy population (~58.15%) in normal fibroblasts. Adding siULK1 offered some protection against doxorubicin's effects on fibroblasts by reducing the number of necrotic cells nearly in half (~16.1%) and significantly increasing the proportion of healthy cells to 68.65% (P~0.001). Knocking down USP20 provided even greater protection, significantly increasing the number of healthy cells up to 77.1% (with P~0.005) (Fig. S1).

Different cancer cell lines reacted differently to doxorubicin therapy. For example, it caused glioblastoma U87 cells to undergo apoptosis (late apoptotic population ~35.83%), and the healthy population significantly decreased to 45.6% (P~0.013). However, when siULK1 and siUSP20 were added, these cells developed some resistance to doxorubicin, and the number of healthy cells rose, reaching up to 50.9% (Fig. S4). Notably, HepG2 cells responded to doxorubicin by activating necrosis (the necrotic population accounting for 15.15%) and suppressing apoptosis, with the apoptotic population accounting for only 5.6% among all populations. Combining the drug with siULK1 or siUSP20 made HepG2 cells more vulnerable to it and significantly increased the number of apoptotic cells (Fig. S5).

The responses of BC cell lines MCF-7 and MDA-MB-231 to doxorubicin also varied. The highest concentration of doxorubicin given to MCF-7 cells significantly promoted both apoptotic and necrotic pathways, resulting in a survival rate of only 33.6%. Interestingly, knocking down USP20 enhanced the effects of chemotherapy and increased the cell necrosis population up to 49.9% compared with the chemotherapy-only group (~22.6%), while knocking down ULK1 allowed the cells to resist the effects of doxorubicin and become more resistant to apoptosis and necrosis, with population sizes reduced to nearly ~16.5 and 10.1% (Fig. S7), respectively. On the other hand, combining siULK1 with doxorubicin made MDA-MB-231 cells markedly more sensitive to the drug, with the apoptotic population increased up to 46.4% compared with the apoptotic population of doxorubicin only (~38.07%). However, USP20 knockdown had no noticeable effect on these cells, and doxorubicin's impact remained unchanged (Fig. S9).

Cisplatin treatment of A549 cells activated the apoptotic cell death pathway dramatically. The healthy population decreased significantly (P<0.0001), while the early and late apoptotic populations increased, with values equal to 16.1 and 24.57%, respectively. Silencing ULK1, along with cisplatin, changed how these cells behaved. They became more sensitive to cisplatin, which decreased the healthy population up to 38.7%, while the healthy population of cisplatin-treated cells reached up to 56.03%. It also increased the late apoptotic population significantly up to 35.1%, with a P<0.0001 when compared with the cisplatin-treated group. Treating A549 cells with siUSP20 and cisplatin also made them vulnerable to the drug and significantly increased the population of late apoptosis up to 30.56% with a P<0.0001, compared with the cisplatin-treated group (Fig. S6). Normal fibroblasts were also affected by cisplatin treatment, as the apoptotic pathway was activated in these cells as well, raising the early apoptotic population significantly up to 22.95% with a P=0.0008. Adding siULK1 to cisplatin-treated fibroblasts protected them from the drug's effects and significantly reduced early cellular apoptosis to a value reaches 11.65% (Fig. S2). Interestingly, normal fibroblasts became more resistant to cisplatin when USP20 was silenced, and their population values were very close to those in the control group.

Table VII. Effect of combination therapy on the induction or inhibition of apoptosis in different cancer cell lines.

Normal Fibroblast-Treated with Doxorubicin

Treatment groups	Control	1.5 IC50 of Dox	P-value	IC50 of Dox	P-value	1.5 IC50 of Dox + siULK1	P-value	IC50 of Dox + siULK1	P-value	1.5 IC50 of Dox + siUSP20	P-value	IC50 of Dox + siUSP20	P-value	1.5 IC50 of Dox + siSCR	P-value	IC50 of Dox + siSCR	P-value
Q1 (Necrosis)	2.15± 0.07	30.25± 2.19	0.003[b]	11.2± 0.99	0.006[b]	16.1± 1.41	0.01[a]	7.95± 1.76	0.15	5.15± 1.34	0.005[b]	4±0.28	0.01[a]	14.75± 0.07	0.009[b]	9.6± 1.13	0.27
Q2 (Late apoptosis)	4.05± 0.21	8.45± 1.06	0.02[a]	10.6± 1.4	0.02[a]	9.4± 0.56	0.38	9.4± 0.99	0.42	8.0± 0.14	0.61	7.85± 1.06	0.15 ns	7.5± 1.13	0.47	8.95± 1.06	0.31
Q3 (Healthy)	90± 0.71	58.15± 0.21	0.0003[c]	59.3± 0.71	0.0005[c]	68.65± 0.49	0.001[b]	76.95± 1.2	0.003[b]	77.1± 1.83	0.004[b]	83.4± 1.41	0.002[b]	73.3± 1.27	0.003[b]	74.95± 2.75	0.016[a]
Q4 (Early apoptosis)	3.8± 0.42	3.2± 0.85	0.46	18.9± 3.11	0.02[a]	5.7± 1.13	0.12	5.7± 1.97	0.03[a]	9.75± 0.35	0.009[b]	4.75± 0.63	0.02	4.35± 0.21	0.20	6.5± 2.82	0.053

Normal Fibroblast-Treated with Cisplatin

Treatment groups	Control	1.5 IC50 of Cis	P-value	IC50 of Cis	P-value	1.5 IC50 of Cis + siULK1	P-value	IC50 of Cis + siULK1	P-value	1.5 IC50 of Cis + siUSP20	P-value	IC50 of Cis + siUSP20	P-value	1.5 IC50 of Cis + siSCR	P-value	IC50 of Cis + siSCR	P-value
Q1 (Necrosis)	2.15± 0.07	0.7± 0.14	0.005[b]	0.9± 0.63	0.02[a]	1.95± 0.63	0.11	2.05± 0.54	0.18	4.05± 0.21	0.002[b]	1.85± 0.07	0.04[a]	1.35± 0.07	0.397	1.4± 0.0	0.12
Q2 (Late apoptosis)	4.05± 0.21	11.2± 0.98	0.006[b]	8.05± 1.06	0.04[a]	8.85± 1.06	0.051	7.5± 0.73	0.77	5.65± 0.63	0.01[a]	6.55± 0.49	0.24	8.9± 0.70	0.03[a]	8.35± 0.35	0.76
Q3 (Healthy)	90± 0.71	65.15± 2.61	0.002[b]	71.4± 0.39	0.007[b]	77.6± 0.39	0.01[a]	79.2± 1.26	0.057	84.85± 0.49	0.002[b]	87.25± 1.76	0.009[b]	82.25± 1.62	0.004[b]	84.55± 1.34	0.01[a]
Q4 (Early apoptosis)	3.8± 0.42	22.95± 1.34	0.002[b]	19.6± 1.3	0.01[a]	11.65± 1.3	0.02[a]	11.25± 2.08	0.076	5.45± 0.35	0.0009[c]	4.35± 1.34	0.014[a]	7.55± 0.77	0.001[b]	5.7± 0.98	0.01[a]

Table VII. Continued.

Normal Fibroblast-Treated with Gemcitabine

Treatment groups	Control	1.5 IC50 of Gem	P-value	IC50 of Gem	P-value	1.5 IC50 of Gem + siULK1	P-value	IC50 of Gem + siULK1	P-value	1.5 IC50 of Gem + siUSP20	P-value	IC50 of Gem + siUSP20	P-value	1.5 IC50 of Gem + siSCR	P-value	IC50 of Gem + siSCR	P-value
Q1 (Necrosis)	2.15± 0.07	0.5± 0.16	0.03[a]	0.8± 0.26	0.04[a]	1.0± 0.31	0.06ns	1.2± 0.54	0.07	1.55± 0.97	0.02[a]	1.2± 0.06	0.0524	1.9± 0.14	0.07	2.05± 1.2	0.55
Q2 (Late apoptosis)	4.05± 0.21	4.3± 1.31	0.51	6.6± 0.61	0.06ns	8.7± 0.84	0.001[b]	7.1± 0.13	0.097	5.85± 0.15	0.239	7.0± 0.14	0.53ns	6.65± 1.34	0.38ns	5.65± 0.63	0.08
Q3 (Healthy)	90± 0.71	64± 0.97	<0.0001[d]	75.8± 2.1	0.0004[c]	82.2± 1.3	<0.0001[d]	83.9± 1.26	0.0001[c]	77.4± 0.19	<0.0001[d]	83.1± 0.27	0.0002[c]	85.85± 1.76	0.0004[c]	87.15± 0.78	0.0008[c]
Q4 (Early apoptosis)	3.8± 0.42	31.2± 1.01	<0.0001[d]	16.8± 0.99	0.0003[c]	8.2± 2.06	<0.0001[d]	7.8± 1.05	<0.0001[d]	15.2± 0.98	<0.0001[d]	8.7± 0.04	<0.0001[d]	5.65± 0.63	<0.0001[d]	5.1± 1.13	0.0006[c]

U87-Treated with Doxorubicin

	Control	1.5 IC50 of Dox	P-value	IC50 of Dox	P-value	1.5 IC50 of Dox + siULK1	P-value	IC50 of Dox + siULK1	P-value	1.5 IC50 of Dox + siUSP20	P-value	IC50 of Dox + siUSP20	P-value	1.5 IC50 of Dox + siSCR	P-value	IC50 of Dox + siSCR	P-value
Q1 (Necrosis)	3.3± 0.28	8.53± 4.19	0.1431	4.5± 0.99	0.2411	12.25± 0.92	0.5760	5.75± 0.78	0.2954	8.9± 0.99	0.6997	4.2± 0.42	0.7317	5.55± 2.33	0.2989	2.65± 2.61	0.4484
Q2 (Late apoptosis)	11.4± 2.82	35.83± 2.67	0.018[a]	30.2± 0.57	0.012[a]	31.85± 2.05	0.33	31.2± 1.56	0.48	25.95± 1.2	0.035[a]	23.7± 1.56	0.03[a]	37.75± 0.07	0.51	27.3± 11.45	0.75
Q3 (Healthy)	70± 2.97	45.6± 2.27	0.013[a]	53.75± 0.35	0.01[a]	50.85± 1.06	0.117	55.35± 1.91	0.364	57.2± 0.14	0.027[a]	61.3± 2.12	0.038[a]	45.6± 3.25	0.874	55.1± 12.02	0.88
Q4 (Early apoptosis)	15.3± 0.14	10.03± 1.78	0.007[b]	11.55± 0.07	0.0009[c]	5.1± 1.84	0.10 ns	7.65± 0.35	0.004[b]	7.95± 0.35	0.21	10.75± 1.06	0.39	11.15± 0.78	0.11	14.95± 2.19	0.15

HepG2-Treated with Doxorubicin

	Control	1.5 IC_{50} Dox	P-value	IC_{50} Dox	P-value	1.5 IC50 of Dox + siULK1	P-value	IC50 of Dox + siULK1	P-value	1.5 IC50 of Dox+ siUSP20	P-value	IC50 of Dox + siUSP20	P-value	1.5 IC50 of Dox + siSCR	P-value	IC50 of Dox + siSCR	P-value
Q1 (Necrosis)	4.55± 1.62	15.15± 0.35	0.0004[c]	14.95± 0.07	0.0004[c]	18.15± 0.21	0.01[b]	12.02± 1.06	0.061	9.53± 2.28	0.022[a]	7.4± 0.45	0.002[b]	5.44± 1.42	0.002[b]	5.4± 2.17	0.007[b]

Table VII. Continued.

HepG2-Treated with Doxorubicin

	Control	1.5 IC_{50} Dox	P-value	IC_{50} Dox	P-value	1.5 IC50 of Dox + siULK1	P-value	IC50 of Dox + siULK1	P-value	1.5 IC50 of Dox+ siUSP20	P-value	IC50 of Dox + siUSP20	P-value	1.5 IC50 of Dox + siSCR	P-value	IC50 of Dox + siSCR	P-value
Q2 (Late apoptosis)	7.1± 1.27	5.65± 0.63	0.24	4.6± 0.28	0.062	10.35± 0.07	0.009[b]	15.55± 0.63	0.002[b]	17.23± 3.86	0.028	13.83± 0.4	0.0001[c]	11.46± 0.55	0.092	12.2± 1.05	0.002[b]
Q3 (Healthy)	82.55± 3.32	77.65± 0.21	0.066	79.45± 0.49	0.173	68.4± 0.28	0.018[a]	55.1± 0.28	0.0003[c]	57.9± 3.84	0.006[b]	65.56± 0.62	0.0001[c]	75.8± 0.56	0.999	71.86± 1.01	0.002[b]
Q4 (Early apoptosis)	5.8± 0.42	1.55± 0.49	0.0011[b]	1± 0.28	0.0004[c]	3.1± 0.14	0.051	17.3± 0.14	0.0002[c]	15.4± 0.26	<0.0001[d]	13.16± 0.37	<0.0001[d]	7.2± 1.06	0.006[b]	10.53 0.32	<0.0001[d]

A549-Treated with Cisplatin

	Control	1.5 IC_{50} DoxP-value		IC_{50} DoxP-value		1.5 IC50 of Dox + siULK1P-value		IC50 of Dox + siULK1P-value		1.5 IC50 of Dox+ siUSP20P-value		IC50 of Dox + siUSP20P-value		1.5 IC50 of Dox + siSCRP-value		IC50 of Dox + siSCR	P-value
Q1 (Necrosis)	0.9± 0.14	3.3± 0.2	0.0083[b]	11.73± 0.83	<0.001[c]	4.5± 0.42	0.0321[a]	5.2± 0.14	0.032[a]	11.53± 0.55	<0.0001[d]	7.45± 0.49	0.018[a]	7.9± 2.5	0.0143	9.4± 4.42	0.9456
Q2 (Late apoptosis)	3.1± 0.07	24.57± 0.25	<0.0001[d]	26.6± 0.95	<0.0001[d]	14.8± 0.77	0.0002[c]	12.05± 0.21	0.0001[c]	30.56± 0.60	0.0009[c]	33.1± 0.28	0.0009[c]	23.63± 1.91	0.44	21.9± 1.34	0.003[b]
Q3 (Healthy)	82.55± 3.32	56.03± 0.31	<0.0001[d]	55.13± 0.8	<0.0001[d]	59.1± 0.57	0.039[a]	67.55± 0.49	0.007[b]	51.26± 0.47	0.029[a]	49.8± 0.26	0.033[a]	58.46± 3.02	0.347	58.36± 4.67	0.5986
Q4 (Early apoptosis)	5.8± 0.42	16.1± 0.26	<0.0001[d]	6.53± 1.3	0.013[a]	21.7± 0.21	0.0002[c]	15.2± 0.14	0.031[a]	6.63± 1.01	<0.0001[d]	9.65± 0.07	0.0489[a]	10± 0.9	0.0002[c]	10.33± 4.5	0.298

MCF-7-Treated with Doxorubicin

	Control	1.5 IC50 of Dox	P-value	IC50 of Dox	P-value	1.5 IC50 of Dox + siULK1	P-value	IC50 of Dox + siULK1	P-value	1.5 IC50 of Dox + siUSP20	P-value	IC50 of Dox + siUSP20	P-value	1.5 IC50 of Dox + siSCR	P-value	IC50 of Dox + siSCR	P-value
Q1 (Necrosis)	4.16± 0.6	22.6± 3.4	0.0004[c]	19.16± 3.5	0.0013	10.05± 4.1	0.006[b]	5.2± 0.14	0.043[a]	49.93± 1.05	0.0001[c]	39.23± 2.77	0.0003[c]	10± 0.28	0.006[b]	10.5± 1.83	0.058
Q2 (Late apoptosis)	2.53± 1.1	40.9± 5.03	0.0001[c]	30.06± 5.9	0.0006[c]	16.5± 7.4	0.002[b]	12.05± 0.21	0.121	35.16± 1.51	0.462	26.26± 2.01	0.754	46.55± 0.91	0.602	38.4± 1.13	0.141

Table VII. Continued.

MCF-7-Treated with Doxorubicin

	Control	1.5 IC50 of Dox	P-value	IC50 of Dox	P-value	1.5 IC50 of Dox + siULK1	P-value	IC50 of Dox + siULK1	P-value	1.5 IC50 of Dox + siUSP20	P-value	IC50 of Dox + siUSP20	P-value	1.5 IC50 of Dox + siSCR	P-value	IC50 of Dox + siSCR	P-value
Q3 (Healthy)	77.06± 2.7	33.56± 5.62	0.0001[c]	47.4± 4.2	0.0003[c]	66.5± 5.7	0.0004[c]	67.55± 0.49	0.004[b]	14.7± 1.21	0.004[b]	33.8± 2.17	0.003[b]	37.8± 1.27	0.907	46.7± 1.83	0.84
Q4 (Early apoptosis)	16.2± 1.4	2.9± 5.6	0.0001[c]	3.4± 1.5	0.0001[c]	2.6± 2.16	0.051ns	15.2± 0.14	0.12	0.121± 0.003	0.012[a]	0.7± 0.1	0.042[a]	5.7± 0.56	0.182	4.45± 1.20	0.906

PanC1-Treated with Gemcitabine

	Control	1.5 IC50 of Gem	P-value	IC50 of Gem	P-value	1.5 IC50 of Gem + siULK1	P-value	IC50 of Gem+ siULK1	P-value	1.5 IC50 of Gem+ siUSP20	P-value	IC50 of Gem + siUSP20	P-value	1.5 IC50 of Gem+ siSCR	P-value	IC50 of Gem + siSCR	P-value
Q1 (Necrosis)	3.05± 0.91	4.6± 0.84	0.652	6.16± 1.75	0.139	14.6± 2.96	0.005[b]	7.36± 0.28	0.991	4.75± 1.06	0.99	10.6± 0.2	0.044[a]	7.03± 1.15	0.490	4.4± 1.27	0.681
Q2 (Late apoptosis)	19± 1.13	32.8± 0.42	0.004[b]	28.8± 2.61	0.0106[a]	36.1± 0.84	0.03[a]	36.1± 5.16	0.043[a]	31.75± 2.05	0.98	33± 0.6	0.391ns	32± 2.26	0.998	34.9± 0.42	0.137
Q3 (Healthy)	71.6± 1.27	55.7± 0.28	0.006[b]	56.43± 3.64	0.005[b]	46.15± 1.34	0.006[b]	49.76± 2.75	0.044	55.85± 0.07	0.999	52.85± 0.25	0.519ns	55.06± 2.41	0.999	55.65± 2.05	0.80
Q4 (Early apoptosis)	6.35± 0.77	6.9± 1.55	0.699ns	7.9± 1.75	0.651	3.15± 0.77	0.039[a]	6.76± 2.68	0.51	7.75± 1.06	0.99	3.55± 0.15	0.045[a]	5.9± 0.65	0.99	5.05± 0.35	0.29

MDA-MB-231-T

	Control	1.5 IC50 of Dox	P-value	IC50 of Dox	P-value	1.5 IC50 of Dox + siULK1	P-value	IC50 of Dox + siULK1	P-value	1.5 IC50 of Dox + siUSP20	P-value	IC50 of Dox + siUSP20	P-value	1.5 IC50 of Dox + siSCR	P-value	IC50 of Dox + siSCR	P-value
Q1 (Necrosis)	5.25± 0.35	16.72± 2.29	0.013[a]	13.8± 1.83	0.030[a]	10.3± 1.27	0.083	17± 0.42	0.13	14.6± 1.55	0.998	17.1± 1.13	0.12	22.5± 3.53	0.086	12.6± 0.42	0.99
Q2 (Late apoptosis)	3.8± 0.28	38.07± 0.17	<0.0001[c]	35± 0.84	0.0001[c]	46.4± 0.14	0.001[b]	40.15± 1.34	0.028[a]	38.65± 1.62	0.66	35.05± 0.91	0.96	32.73± 2.75	0.053	26.55± 1.2	0.014[a]

Table VII. Continued.

MDA-MB-231-T															
	Control	1.5 IC50 of Dox	P-value	IC50 of Dox	P-value	1.5 IC50 of Dox + siULK1	P-value	IC50 of Dox + siULK1	P-value	1.5 IC50 of Dox + siUSP20	P-value	IC50 of Dox + siUSP20	P-value	1.5 IC50 of Dox + siSCR	P-value	IC50 of Dox + siSCR	P-value
Q3 (Healthy)	85.8± 0.42	36.62± 1.37	0.0004[b]	34.45± 1.06	0.0002[c]	24.1± 1.55	0.013[a]	30± 0.28	0.02[a]	38.8± 0.70	0.18	36.9± 1.9	0.26	37± 1.62	0.76	44.5± 3.39	0.057
Q4 (Early apoptosis)	5.15± 0.49	8.57± 0.74	0.032[a]	16.75± 2.05	0.006[b]	19.65± 0.63	0.003[b]	12.85± 1.48	0.18	7.95± 0.63	0.94	10.9± 0.07	0.057	7.73± 2.4	0.85	16.4± 1.69	0.86

Each treatment group displays the results of three experimental repeats. Data was analyzed using one-way ANOVA followed by Bonferroni's multiple comparisons post hoc test to compare each quartile of combination therapy group with the corresponding quartile in the chemotherapy only treatment group. [a]P<0.05, [b]P<0.01, [c]P<0.001 and [d]P<0.0001.

Gemcitabine also had a mild effect on normal cells and triggered the early apoptotic pathway. However, when gemcitabine treatment was combined with siULK1 or siUSP20, fibroblasts became resistant to gemcitabine. This was shown by an increase in healthy populations (up to 82.2 and 77.4% for both treatment groups, respectively) and a decrease in early and late apoptotic cells (Fig. S3). When gemcitabine was added to PanC1 cancer cells, it significantly activated the apoptotic pathway and increased the late apoptotic population up to 32.8%, with a P~0.003. Yet, when gemcitabine was combined with siULK1, PanC1 cells became more sensitive, leading to a higher number of cells undergoing late apoptosis (accounting for 36.1%, with P~0.03). Silencing USP20 did not significantly affect the outcome for gemcitabine-treated PanC1 cells, and the cell responses matched those seen in the gemcitabine-treated group (Fig. S8).

Discussion

Autophagy is a homeostasis maintenance mechanism that aims to prevent the accumulation of damaged cellular components or compartments and maintain cellular balance. Besides its canonical functions in the cell, it is well known to have several noncanonical functions that affect numerous vital cellular responses (24). In cancers, it has been postulated that autophagy plays an important role in reprogramming the cell, modulating cellular responses to chemotherapy and determining cellular fate, either survival or death. However, the available data were controversial and the effect of autophagy on cancer progression and therapy effectiveness was not the same for different cancer types and remained unclearly defined. At present, to the best of our knowledge, the data that precisely dissect the functional classification of autophagy in different cancer types are still lacking and need to be further clarified. The aim of the present study was to uncover the functional role of autophagy in a number of cancer cell lines by specifically evaluating its role in cancer cell fate and its responses to the conventional chemotherapeutic agents. Direct evidence that autophagy is differentially modulated in different cancer cell lines for the sake of cancer survival was provided. Powerful evidence was also presented that autophagy inhibition is directly correlated with cancer cellular fates by being a cytoprotective or cytotoxic mechanism. Furthermore, the precise correlation between autophagy inhibition and the desensitization or resensitization of different investigated cancer cells toward conventional therapies was determined. Furthermore, it has been successfully validated that the autophagy-related initiation factor, ULK1, and its de-ubiquitinase stabilizing enzyme, USP20, are powerful potential targets for the treatment of cancers. ULK1 was selected as the central autophagy reference molecule because of its established, indispensable role in initiating the autophagy cascade. USP20 was chosen as a parallel target because of its potential but understudied role as a de-ubiquitinase that may regulate ULK1 turnover and activity, thereby revealing a novel post-translational mechanism that could reshape the understanding of autophagy regulation.

The data of the present study demonstrated that ULK1 and USP20 expression varies among cancer cells, with either low or high expression levels. Among the tested cells, ULK1

was mostly expressed in the MCF-7 BC cell line, while the minimum expression was detected in U87 glioblastoma cells. This variability in the expression reflects the different dependence of cancer cells on the autophagy pathway and may relate to chemoresistance, metastasis and the fate of the cells. The data of the present study are in line with other studies, where it has been previously postulated that ULK1 is overexpressed in MCF-7 cells, while lowly expressed in MDA-MB-231 cells (25). It has been indicated that overexpression of ULK1 is conversely correlated with the prognosis in a number of cancer types, including BC (26). Interestingly, low expression of ULK1 in MDA-MB231 has been correlated with more metastatic behavior, while overexpression of ULK1 appears to be protective against metastasis. This is because ULK1 is required to phosphorylate and inhibit Exo70, an essential component of the exocyst complex, which is necessary for invasion and metastasis (25). However, this differential expression of ULK1 appears to affect the sensitivity of cancer cells to doxorubicin. In the MCF-7 cell line, the high expression level of ULK1 confers greater sensitivity to doxorubicin compared with the MDA-MB-231 cell line. However, when ULK1 was suppressed, MCF-7 cells exhibited more aggressive behavior and became desensitized to the drug. On the other hand, MDA-MB-231 is more resistant to doxorubicin when compared with MCF-7 but becomes more vulnerable to the drug when ULK1 is depressed. This can be explained as the minimum level of ULK1 in MDA-MB-231 cells is essential to maintain the aggressive behavior, but when it is suppressed, the cells lose these aggressive traits.

Interestingly, the opposing effects of ULK1 on doxorubicin sensitivity in MCF-7 vs. MDA-MB-231 cells likely reflect its context-dependent roles in autophagy and apoptosis. In MCF-7 cells, high basal ULK1 supports autophagy that facilitates stress-induced apoptosis; therefore knockdown reduces doxorubicin sensitivity. Conversely, in MDA-MB-231 cells, basal autophagy may be primarily cytoprotective, and ULK1 knockdown disrupts this survival mechanism, sensitizing cells to treatment. These differences are influenced by cell-type-specific factors, including p53 status, baseline autophagic flux, and apoptotic wiring, highlighting ULK1 as a versatile regulator whose impact on chemotherapy response is highly context-dependent. Furthermore, a context-dependent approach to ULK1 modulation may be more effective than uniform inhibition. In highly aggressive or metastatic cancers, such as MDA-MB-231, ULK1 and USP20 appear to restrain pro-metastatic programs, suggesting that ULK1 activation could suppress invasion and metastasis. Conversely, in tumors where ULK1 supports cytoprotective autophagy, inhibition may enhance chemosensitivity. Therefore, therapeutic strategies should be guided by cell-type-specific autophagy dependency, basal ULK1/USP20 expression and metastatic potential, with activation or inhibition tailored to exploit the tumor's particular vulnerabilities while minimizing harm to normal tissues.

Tang *et al* (27) previously reported that ULK1 is overexpressed in non-small cell lung cancer cells (NSCLC), compared with normal lung cells and this is correlated with poor prognosis and patients' survival rate. Inhibition of ULK1 with SBI0206965, a selective ULK1 inhibitor, reversed the aggressive trait of these cells and sensitized cells to cisplatin. The data of the present study showed different outcomes, as ULK1 appears to prevent the progression of the disease, and when it is inhibited, A549 cells become more aggressive and resistant to cisplatin. However, the correlation between ULK1 and drug-resistant genes must be further investigated to understand the mechanism underlying these results. The apparent contradiction between the present study's findings in A549 cells and those reported by Tang *et al* (27) likely reflects differences in both inhibition strategy and cellular context. Tang *et al* (27) employed the small-molecule ULK1 inhibitor SB10206965, which may affect ULK1 kinase activity without fully depleting protein levels or disrupting its scaffolding functions, whereas siRNA-mediated knockdown was used in the present study, leading to a more complete loss of ULK1 protein and potentially broader effects on autophagy-independent roles such as mitotic regulation. Additionally, NSCLC encompasses heterogeneous subtypes with distinct basal autophagy flux, stress-response pathways and genetic backgrounds, all of which can influence the outcome of ULK1 inhibition on cisplatin sensitivity. Taken together, these methodological and biological differences likely account for the divergent results and underscore the context-dependent nature of ULK1 function in chemotherapy response.

USP20 has been positively correlated to the development and progression of cancers. It has been reported that USP20 is differentially expressed between cancer and normal cells, being highly expressed in most cancers compared with their corresponding normal cells but found to be lowly expressed in a few cancer types, including pancreatic cancers (28). Inconsistent with the previous findings, the results of the present study are similar in the context of USP20 expression level. Moreover, it has been reported that USP20 is responsible for the stabilization of the labile SNAI2/SLUG, which is a transcription factor that drives invasion and metastasis in cancers (29). When USP20 was inhibited, SNAI2/SLUG was subjected to degradation after being ubiquitinated, which in turn inhibited tumor progression (29). Consistently, the results of the present study indicate that USP20 inhibition re-sensitized numerous cancer types to their corresponding chemotherapies, including MCF-7, HepG2, A549 and PanC1, and enhanced the effectiveness of the chemotherapy. By contrast, the triple-negative MDA-MB-231 BC and U87 glioblastoma cell lines behaved differently, as they remained unchanged or became highly resistant to doxorubicin, respectively. Overall, USP20 knockdown sensitizes MCF-7 cells but not MDA-MB-231 cells, likely reflecting cell-type-specific dependencies. The highly metastatic, triple-negative MDA-MB-231 cells may rely on USP20-independent pathways to maintain survival and invasion, using alternative de-ubiquitinases or signaling networks to stabilize pro-metastatic factors like SNAI2/SLUG. This highlights the context-dependent role of USP20 and the plasticity of survival mechanisms in aggressive BC. A comprehensive proteomic, metabolomic, and transcriptomic study must be performed to widen the understanding of the mechanisms underlying ULK1 and USP20 modulation and the chemotherapeutic sensitivity of different cancer cell lines.

The present study determined whether chemotherapeutic medications alter autophagy-related genes including P62, USP20 and ULK1. In liver cancer HepG2 cells and glioblastoma U87 cells, doxorubicin treatment leads to downregulation

of ULK1 and USP20 expression levels and the overexpression of P62, suggesting the inhibition of autophagy. Although autophagy induction is a well-described response to chemotherapeutic stress, the present findings indicated that doxorubicin can also suppress autophagy in a cell-type-dependent manner, as reflected by ULK1 downregulation and p62 accumulation in HepG2 and U87 cells. These seemingly opposing outcomes can be reconciled by recognizing that chemotherapy produces biphasic and context-specific autophagy responses. At early or lower doses, genotoxic stress typically activates p53-, NF-κB-, and MAPK-driven transcriptional programs that stimulate autophagy as a cytoprotective mechanism. However, prolonged or high-dose exposure can overwhelm cellular proteostasis, impair lysosomal function, or promote ULK1 degradation, resulting in blocked autophagic flux despite transcriptional activation of stress-responsive genes. Thus, doxorubicin may either induce or inhibit autophagy depending on dose, timing, and the intrinsic stress-response architecture of each cell line, explaining why HepG2 and U87 exhibit autophagy suppression while other models demonstrate induction. Interestingly, the observations made in the present study suggested that in U87 glioblastoma cells, basal autophagy maintained by ULK1 and USP20 may be pro-death rather than cytoprotective. Inhibition of these autophagy regulators reduces stress-induced autophagic activity, which in this context appeared to facilitate doxorubicin-induced apoptosis. Consequently, knockdown of ULK1 or USP20 diminishes pro-death autophagy, allowing cells to survive chemotherapy, consistent with the notion that the functional outcome of autophagy is highly context- and cell-type-dependent. These findings highlight that in aggressive cancer types such as glioblastoma, basal autophagy can act as a tumor-suppressive, pro-apoptotic mechanism.

According to Sha *et al* (30), an elevated P62 level indicates a compromised proteasomal function in cells. Moreover, doxorubicin treatment markedly increased the level of P62 transcripts in MDA-MB-231, indicating that autophagy is being inhibited in the cells, but it did not affect the expression of ULK1 or USP20. These findings could be explained by the fact that autophagy occurs through a variety of routes inside the cell and that autophagy-mediating factors other than ULK1 and USP20, including ATG12 and ATG7, may be downregulated in response to the drug. Another research group demonstrated that chemotherapy treatment of liver cancer HepG2 cells increases autophagy flux, dictated by an increase in LC3II level (31). Their outcome contradicts the findings of the present study; however, the chemotherapeutic agents evaluated in their study were 5-fluorouracil and cisplatin, but not doxorubicin, which was used in the present study, suggesting that different chemotherapies operate with different mechanisms.

Chemotherapeutic agents such as doxorubicin and cisplatin appear to transcriptionally upregulate ULK1, USP20, and P62 through activation of stress-responsive signaling pathways. Both drugs induce substantial DNA damage, oxidative stress and ER stress, which activate transcription factors including p53, NF-κB, ATF4/CHOP and Nrf2. These regulators are well known to drive the expression of autophagy-related genes as part of a compensatory cytoprotective response. In parallel, activation of the DNA damage-response kinases (ATM/ATR) and MAPK pathways further enhances transcription of autophagy initiation factors and stress adaptors. As a result, doxorubicin and cisplatin promote a coordinated upregulation of ULK1, USP20, and P62 to enhance autophagy and maintain cellular homeostasis under chemotherapeutic stress.

Cisplatin was confirmed to induce ULK1 expression in lung cancer A549 cells, and this elevation was correlated with poor prognosis and the development of the cisplatin-resistant trait. When ULK1 was knocked down, A549 became sensitized to cisplatin and underwent apoptosis (27). Conversely, the highest tested concentration of cisplatin in the present research did not affect ULK1 expression, accompanied by an elevation of P62 expression, indicating an impaired autophagy process. When ULK1 was knocked down, resistance to cisplatin was developed. Suggesting that the presence of ULK1 and a functional autophagy process is important for effective chemotherapy treatment. Interestingly, USP20 becomes elevated upon cisplatin employment in A549 cells. It has been indicated that USP20 high levels promote cell proliferation, migration and invasion, and are directly correlated with poor prognosis and survival rates (22). These data are in line with our data, as USP20 knockdown leads to higher sensitivity of A549 to cisplatin.

Regarding the pancreatic PanC1 cells, gemcitabine chemotherapy massively induced ULK1 expression. However, the induction of autophagy in this case appears to be important for PanC1 survival after their exposure to gemcitabine, evidenced by the enhanced sensitivity of PanC1 to the drug after siULK1 administration. Accordingly, one research group indicated that gemcitabine acts by inhibiting the replication of DNA and inducing its damage, and as a survival response, PanC1 cells induced autophagy and the lysosomal functions upon drug exposure (32). The therapeutic efficiency of this drug is highly limited due to the development of drug resistance by the growing pancreatic cancers (33). Seemingly, PanC1 develops this resistance by inducing autophagy as a survival mechanism to recycle gemcitabine-induced damage in the cellular components and enhance cell growth (34). Thus, inhibiting autophagy along with gemcitabine administration may enhance therapeutic effectiveness against the disease.

Although the present study focused on single-agent chemotherapy, ULK1/USP20 modulation could influence combination therapies in a context-dependent manner. Inhibiting ULK1/USP20 may sensitize tumor cells to targeted therapies by blocking cytoprotective autophagy, while activating ULK1 in pro-death contexts could enhance immunotherapy by promoting immunogenic cell death. Careful consideration of tumor subtype, basal autophagic flux, and immune status will be essential to optimize such combination strategies.

The fate of cancer cells when they are exposed to chemotherapeutic treatment is governed by the complicated relationship between apoptosis and autophagy, processes that may operate synergistically or antagonize each other (35). Apoptosis is initiated by extrinsic ligands or intrinsic cellular stresses, such as reactive oxygen species, DNA damage and mitochondrial stress (36). The balance between the BCL-2 family proteins, mainly the proapoptotic protein Bax and the antiapoptotic protein BCL-2, dictates the fate of the cell, either survival or death (37). However, studies that investigate the correlation between ULK1, USP20, and apoptosis in cancers

are contradictory and minimal, especially for USP20. For this aim, the dynamic relationship between the autophagy-related gene, ULK1, the de-ubiquitinating enzyme USP20, and apoptosis is further clarified in the present study. Although autophagy is widely known to antagonize apoptotic cell death, it can operate hand in hand with apoptosis, specifically after persistent exposure to stressful conditions (35). This contradictory function of autophagy over apoptotic proteins can be observed in the present study. When ULK1 was inhibited in the investigated cancer cell lines, the latter showed variable responses regarding apoptosis induction. Chemotherapeutic agents also show different patterns and magnitudes in inducing apoptosis and exhibit different mechanisms that drive cellular death.

Accordingly, knockdown of ULK1 or USP20 likely disrupts autophagic homeostasis, leading to the accumulation of damaged organelles and cellular stress, which can trigger the intrinsic apoptotic pathway. Specifically, autophagy inhibition may promote mitochondrial dysfunction, resulting in the release of cytochrome c and subsequent activation of pro-apoptotic proteins such as Bax, while suppressing anti-apoptotic Bcl-2, thereby shifting the Bax/Bcl-2 ratio in favor of apoptosis. This mechanistic link is consistent with prior reports demonstrating that impaired autophagy sensitizes cells to mitochondrial mediated apoptosis. Furthermore, doxorubicin induces cellular apoptosis in BC cell lines, MCF-7 and MDA-MB-231, and the glioblastoma U87 cell line. On the contrary, doxorubicin treatment of liver cancer HepG2 cells inhibited the apoptotic pathway but enhanced the necrotic pathway. Necrosis is another uncontrolled cell death mechanism, which involves molecular mechanisms other than Bax and Bcl-2 (38).

Knockdown of USP20 also shows variable effects on cancerous cells' fate. In a previous study, the knockdown of USP20 in the HeLa cervical cancer cell line promoted cellular survival and growth by stabilizing P62, and activating the TNFα/NF-κB survival pathway (39). When USP20 was depleted, apoptosis was induced in HeLa cells (39). Furthermore, USP20 prevents the lysosomal degradation of ULK1 and thus enhances the operation of autophagy under starvation conditions (40), and its depletion reduces autophagy and drives apoptosis (40). These data reflect the complex relationship between these factors and apoptosis, as they may intersect at numerous points within different cellular pathways. Altogether, cancer cell fate after combining chemotherapy with ULK1 or USP20 silencing depends on the dynamic balance between Bax and Bcl-2 triggered by both treatments. Thus, the effect of ULK1 and USP20 silencing on the apoptotic pathway may antagonize and reduce the effectiveness of the conventional chemotherapy in some cancer types but synergize and augment the apoptotic effect of chemotherapies in other cancer cells.

Primary fibroblasts proliferate reliably, maintain a stable karyotype, and are easier to culture than many primary epithelial cells. This ensures reproducible comparisons across experiments. In addition, HDFa cells lack the constitutive stress, metabolic rewiring, and proliferative signaling that often complicate the interpretation of cancer cell lines (41). This makes them a useful baseline for identifying cancer-associated upregulation of proteins such as ULK1 and USP20. ULK1 and USP20 expression are highly tissue-dependent. Some tissues naturally express higher or lower levels of autophagy regulators (42,43). Tissue-matched controls might show that certain cancer cell lines do not overexpress ULK1 or USP20 when compared with their native tissue.

Regarding the therapeutic implications, the context-dependent effects of ULK1 inhibition indicate that careful patient stratification is necessary to achieve a therapeutic window. Tumors with high basal ULK1 expression or elevated autophagic flux may be more dependent on ULK1 for survival, whereas normal tissues with lower flux, such as fibroblasts, may be spared. Additional factors, including p53 status, apoptotic priming, and expression of co-regulators such as USP20, could further refine predictions of ULK1 dependency. Assessing tumor subtype, metastatic potential, and markers of oxidative stress or metabolic rewiring may also help identify cancers that are particularly sensitive to ULK1 inhibition, allowing selective targeting of tumor cells while minimizing toxicity to normal tissue.

While the findings of the present study provide valuable results, some limitations can be addressed. Nevertheless, the involvement of more cell line types would broaden our understanding of the multifaceted role of autophagy. Furthermore, the present study compared the changes in the expression of ULK1 and USP20 in cancer cell lines relative to normal skin fibroblast cells only. However, it would be more accurate to correlate the changes in their expression with the normal cells of the same type as the cancer cells. Another limitation of the present study is that the autophagic flux at the protein level was not directly assessed, as the antibodies for LC3 and p62 tested were non-specific. Therefore, while the mRNA measurements provided insight into transcriptional regulation of autophagy-related genes, they may not fully reflect functional autophagic activity. Additionally, a potential limitation was that siRNA reagents can produce off-target or immune-stimulatory effects. While all knockdowns were compared with a scrambled siRNA control, some residual non-specific effects, such as modest IC_{50} shifts in fibroblasts, cannot be fully excluded and should be considered when interpreting the data.

In conclusion, the present study provided a detailed dataset that reflects the biphasic role of autophagy among different cancer types. ULK1 and USP20 are differentially expressed among different cancer types, and their knockdown is directly correlated with chemoresistance of cancer cells toward the conventional chemotherapeutic drugs. The presented data indicate that different cancer cells react in various ways when ULK1 and USP20 are silenced in the context of cellular death. The available data help us determine where the inhibition of these genes can be incorporated with conventional therapy to improve its effectiveness and where it must be avoided to prevent the development of more aggressive tumor characteristics. Further studies should be conducted to uncover the molecular mechanisms underlying the differential role of autophagy in these cancers, involving a comprehensive metabolomics, transcriptomics, and proteomics analysis. Also, key *in vivo* studies should use xenograft or patient-derived models to test genetic or pharmacologic inhibition of ULK1 and USP20 alongside chemotherapy, assessing tumor growth, apoptosis, and drug response. Metastatic models can determine effects on invasion and metastasis, while toxicity studies ensure safety. Linking

ULK1/USP20 expression and autophagy or apoptosis markers with treatment outcomes will confirm target engagement and support their therapeutic potential.

Acknowledgements

The authors would like to thank Mrs Zain Hindash (Department of Biology, University of Jordan, Amman, Jordan) for technical support.

Funding

The present study was supported by the Deanship of Scientific Research in The University of Jordan (grant no. 2024-172/2023).

Availability of data and materials

The data generated in the present study are included in the figures and/or tables of this article.

Authors' contributions

AI, TA, DA and MZ conseptualized the present study and performed the experimental design. AI and TA performed statistical analysis and drafted the manuscript. All authors read and approved the final version of the manuscript. AI and TA confirm the authenticity of all the raw data.

Ethics approval and consent to participate

Not applicable.

Patient consent for publication

Not applicable.

Competing interests

The authors declare that they have no competing interests.

References

1. Kitada M and Koya D: Autophagy in metabolic disease and ageing. Nat Rev Endocrinol 17: 647-661, 2021.
2. Ahmadi-Dehlaghi F, Mohammadi P, Valipour E, Pournaghi P, Kiani S and Mansouri K: Autophagy: A challengeable paradox in cancer treatment. Cancer Med 12: 11542-11569, 2023.
3. Rakesh R, PriyaDharshini LC, Sakthivel KM and Rasmi RR: Role and regulation of autophagy in cancer. Biochim Biophys Acta Mol Basis Dis 1868: 166400, 2022.
4. Yu L, Chen Y and Tooze SA: Autophagy pathway: Cellular and molecular mechanisms. Autophagy 14: 207-215, 2018.
5. Hama Y, Fujioka Y, Yamamoto H, Mizushima N and Noda NN: The triad interaction of ULK1, ATG13, and FIP200 is required for ULK complex formation and autophagy. Elife 13: RP101531, 2025.
6. Follo C, Vidoni C, Morani F, Ferraresi A, Seca C and Isidoro C: Amino acid response by halofuginone in cancer cells triggers autophagy through proteasome degradation of mTOR. Cell Commun Signal 17: 39, 2019.
7. Sun T, Liu Z and Yang Q: The role of ubiquitination and deubiquitination in cancer metabolism. Mol Cancer 19: 146, 2020.
8. Chakraborty P: Contrasting role of autophagy in different types of cancer: A review toward biomarkers and therapeutic improvement. Biomed Biotechnol Res J 5: 260-266, 2021.
9. Russell RC and Guan KL: The multifaceted role of autophagy in cancer. EMBO J 41: e110031, 2022.
10. Yun CW, Jeon J, Go G, Lee JH and Lee SH: The dual role of autophagy in cancer development and a therapeutic strategy for cancer by targeting autophagy. Int J Mol Sci 22: 179, 2020.
11. Debnath J, Gammoh N and Ryan KM: Autophagy and autophagy-related pathways in cancer. Nat Rev Mol Cell Biol 24: 560-575, 2023.
12. Marinković M, Šprung M, Buljubašić M and Novak I: Autophagy modulation in cancer: Current knowledge on action and therapy. Oxid Med Cell Longev 2018: 8023821, 2018.
13. Ganzleben I, Neurath MF and Becker C: Autophagy in cancer therapy-molecular mechanisms and current clinical advances. Cancers (Basel) 13: 5575, 2021.
14. Mulcahy Levy JM and Thorburn A: Autophagy in cancer: Moving from understanding mechanism to improving therapy responses in patients. Cell Death Differ 27: 843-857, 2020.
15. Mahri S, Villa R, Shiau YP, Tang M, Racacho KJ, Zong Q, Chowdhury SI, Hua T, Godinez F, Birkeland A, *et al*: Nanomedicine approaches for autophagy modulation in cancer therapy. Small Sci 5: 2400607, 2025.
16. Walweel N and Aydin O: Enhancing therapeutic efficacy in cancer treatment: Integrating nanomedicine with autophagy inhibition strategies. ACS Omega 9: 27832-27852, 2024.
17. Zhu L, Li Z, Wang H, Cheng Z and Zhang L: Unraveling the mysterious veil of ULK1: From non-canonical functions to therapeutic applications. Int J Biol Macromol 18: 145177, 2025.
18. Ma L, Li W, Zhang Y, Qi L, Zhao Q, Li N, Lu Y, Zhang L, Zhou F, Wu Y, *et al*: FLT4/VEGFR3 activates AMPK to coordinate glycometabolic reprogramming with autophagy and inflammasome activation for bacterial elimination. Autophagy 18: 1385-1400, 2022.
19. Zhang J, Tripathi DN, Jing J, Alexander A, Kim J, Powell RT, Dere R, Tait-Mulder J, Lee JH, Paull TT, *et al*: ATM functions at the peroxisome to induce pexophagy in response to ROS. Nat Cell Biol 17: 1259-1269, 2015.
20. Deng R, Zhang HL, Huang JH, Cai RZ, Wang Y, Chen YH, Hu BX, Ye ZP, Li ZL, Mai J, *et al*: MAPK1/3 kinase-dependent ULK1 degradation attenuates mitophagy and promotes breast cancer bone metastasis. Autophagy 17: 3011-3029, 2021.
21. Ji X, Zhang X and Li Z: ULK1 inhibitor induces spindle microtubule disorganization and inhibits phosphorylation of Ser10 of histone H3. FEBS Open Bio 10: 2452-2463, 2020.
22. Li Q, Ye C, Tian T, Jiang Q, Zhao P, Wang X, Liu F, Shan J and Ruan J: The emerging role of ubiquitin-specific protease 20 in tumorigenesis and cancer therapeutics. Cell Death Dis 13: 434, 2022.
23. Livak KJ and Schmittgen TD: Analysis of relative gene expression data using real-time quantitative PCR and the 2(-Delta Delta C(T)) method. Methods 25: 402-408, 2001.
24. Wang Y, Wu L and Van Kaer L: Role of canonical and noncanonical autophagy pathways in shaping the life journey of B cells. Front Immunol 15: 1426204, 2024.
25. Mao L, Zhan YY, Wu B, Yu Q, Xu L, Hong X, Zhong L, Mi P, Xiao L, Wang X, *et al*: ULK1 phosphorylates Exo70 to suppress breast cancer metastasis. Nat Commun 11: 117, 2020.
26. Tang J, Deng R, Luo RZ, Shen GP, Cai MY, Du ZM, Jiang S, Yang MT, Fu JH and Zhu XF: Low expression of ULK1 is associated with operable breast cancer progression and is an adverse prognostic marker of survival for patients. Breast Cancer Res Treat 134: 549-560, 2012.
27. Tang F, Hu P, Yang Z, Xue C, Gong J, Sun S, Shi L, Zhang S, Li Z, Yang C, *et al*: SBI0206965, a novel inhibitor of Ulk1, suppresses non-small cell lung cancer cell growth by modulating both autophagy and apoptosis pathways. Oncol Rep 37: 3449-3458, 2017.
28. Wang T, Bai Y, Dong Y, Qin J, Zhou X, Wang A, Liu D, Li X, Ma Z and Hu Y: A comprehensive analysis of deubiquitinase USP20 on prognosis and immunity in pan-cancer. FASEB J 39: e70499, 2025.
29. Li W, Shen M, Jiang YZ, Zhang R, Zheng H, Wei Y, Shao ZM and Kang Y: Deubiquitinase USP20 promotes breast cancer metastasis by stabilizing SNAI2. Genes Dev 34: 1310-1315, 2020.
30. Sha Z, Schnell HM, Ruoff K and Goldberg A: Rapid induction of p62 and GABARAPL1 upon proteasome inhibition promotes survival before autophagy activation. J Cell Biol 217: 1757-1776, 2018.
31. Guo XL, Li D, Hu F, Song JR, Zhang SS, Deng WJ, Sun K, Zhao QD, Xie XQ, Song YJ, *et al*: Targeting autophagy potentiates chemotherapy-induced apoptosis and proliferation inhibition in hepatocarcinoma cells. Cancer Lett 320: 171-179, 2012.

32. Marchand B, Poulin MA, Lawson C, Tai LH, Jean S and Boucher MJ: Gemcitabine promotes autophagy and lysosomal function through ERK-and TFEB-dependent mechanisms. Cell Death Discov 9: 45, 2023.
33. Gillson J, Abd El-Aziz YS, Leck LYW, Jansson PJ, Pavlakis N, Samra JS, Mittal A and Sahni S: Autophagy: A key player in pancreatic cancer progression and a potential drug target. Cancers (Basel) 14: 3528, 2022.
34. Chavez-Dominguez R, Perez-Medina M, Lopez-Gonzalez JS, Galicia-Velasco M and Aguilar-Cazares D: The double-edge sword of autophagy in cancer: From tumor suppression to pro-tumor activity. Front Oncol 10: 578418, 2020.
35. Mariño G, Niso-Santano M, Baehrecke EH and Kroemer G: Self-consumption: The interplay of autophagy and apoptosis. Nat Rev Mol Cell Biol 15: 81-94, 2014.
36. Galluzzi L, Vitale I, Aaronson SA, Abrams JM, Adam D, Agostinis P, Alnemri ES, Altucci L, Amelio I, Andrews DW, *et al*: Molecular mechanisms of cell death: Recommendations of the nomenclature committee on cell death 2018. Cell Death Differ 25: 486-541, 2018.
37. Tang D, Kang R, Berghe TV, Vandenabeele P and Kroemer G: The molecular machinery of regulated cell death. Cell Res 29: 364-374, 2019.
38. Kang S, Kim KR, Cho M, Hwang J, Yang JM, Kim JK and Choi WJ: High-resolution imaging of morphological changes associated with apoptosis and necrosis using single-cell full-field optical coherence tomography. Biosensors (Basel) 15: 522, 2025.
39. Ha J, Kim M, Seo D, Park JS, Lee J, Lee J and Park SH: The deubiquitinating enzyme USP20 regulates the TNFα-induced NF-κB signaling pathway through stabilization of p62. Int J Mol Sci 21: 3116, 2020.
40. Kim JH, Seo D, Kim SJ, Choi DW, Park JS, Ha J, Choi J, Lee JH, Jung SM, Seo KW, *et al*: The deubiquitinating enzyme USP20 stabilizes ULK1 and promotes autophagy initiation. EMBO Rep 19: e44378, 2018.
41. Zhang F, Ma Y, Li D, Wei J, Chen K, Zhang E, Liu G, Chu X, Liu X, Liu W, *et al*: Cancer associated fibroblasts and metabolic reprogramming: Unraveling the intricate crosstalk in tumor evolution. J Hematol Oncol 17: 80, 2024.
42. Wang J, Zheng F, Wang D and Yang Q: Regulation of ULK1 by WTAP/IGF2BP3 axis enhances mitophagy and progression in epithelial ovarian cancer. Cell Death Dis 15: 97, 2024.
43. Jin R, Luo Z, Jun-Li, Tao Q, Wang P, Cai X, Jiang L, Zeng C and Chen Y: USP20 is a predictor of poor prognosis in colorectal cancer and associated with lymph node metastasis, immune infiltration and chemotherapy resistance. Front Oncol 13: 1023292, 2023.